


REVIEW

Open Access



Dissolved organic compounds in geothermal fluids used for energy production: a review

Alessio Leins^{1,2*} , Danaé Bregnard³, Andrea Vieth-Hillebrand¹, Pilar Junier³ and Simona Regenspurg¹

*Correspondence:
alessio.leins@gfz-potsdam.de

¹ GFZ German Research Centre for Geosciences, Telegrafenberg, 14473 Potsdam, Germany

² Institute of Geosciences, Friedrich Schiller University, Burgweg 11, 07749 Jena, Germany

³ Institute of Biology, University of Neuchâtel, Rue Émile-Argand 11, 2000 Neuchâtel, Switzerland

Abstract

Dissolved organic matter (DOM) can be found in a variety of deep subsurface environments such as sedimentary basins, oil fields and mines. However, the origin, composition and fate of DOM within deep geothermal reservoirs used for energy production is relatively unknown. With well depths reaching a few kilometers, these sites give access to investigate deep subsurface environments. Natural DOM as well as artificial DOM (e.g., from chemical scaling inhibitors) might serve as nutrients for microorganisms or affect chemical properties of the fluids by complexation. Its composition might reveal hydraulic connections to organic-rich strata, giving insights to the fluid flow within the reservoir. This review presents an overview of a total of 143 fluid samples from 22 geothermal sites (mainly central Europe), from the literature and compiling data to address the importance of DOM in geothermal fluids and how it might affect geothermal operation. The environmental conditions of the sites included varied greatly. Temperatures range from 34 to 200 °C, depths from 850 to 5000 m, chloride content from 0.1 to 160 g L⁻¹, and dissolved organic carbon (DOC) concentrations from 0.1 to 30.1 g L⁻¹. The DOC concentrations were found to be generally lower in the fluids with temperatures below 80 °C. DOC concentrations were higher in fluids with temperatures above 80 °C and showed a decrease towards 200 °C. Microbial degradation might be the main driver for low DOC concentrations in the lower temperature range (below 80 °C), while thermal degradation likely accounts for the decline in DOC in the temperature region between 80 °C and 200 °C. This review shows that DOM can be found in a variety of geothermal reservoirs and that it could be an additional essential tool to better understand fluid chemistry and reservoir conditions, and to optimize geothermal operation.

Keywords: Geothermal fluids, Brine, Dissolved organic matter, Dissolved organic carbon, Inhibitor, Geothermal energy production

Introduction

Geothermal energy is gaining increasing importance in the alternative energy mix (e.g., solar and wind energy), but one drawback for successfully exploiting geothermal energy is the uncertainty related to chemical reactions of the geothermal fluid that derives from great depths of the earth's crust. Most of the inorganic components in those fluids are well described and their occurrence and reactions relatively well understood by now (see for instance Regenspurg et al. 2016; Sanjuan et al. 2016). Depending on the reservoir

rock formation, fluid circulation, and possible connectivities to other reservoir rocks, the fluids vary in salinity from a few mg L^{-1} (Vetter 2012) to several hundred g L^{-1} (Hanor 1994) and can contain a range of various metals. Fluid–rock interactions may also lead to an enrichment of certain elements, as in the case of formation waters from the Rotliegend sandstone with Na and Ca as the most dominant ones, but also with increasing amounts of, e.g., K, Sr, and Li (Lüders et al. 2010; Moeller et al. 2008; Tesmer et al. 2007).

It is crucial for geothermal energy exploitation to know the exact composition of those fluids in order to predict possible chemical reactions. One of the main problems encountered in geothermal power plants is the precipitation of certain minerals (scaling) in the boreholes, pipes, and equipment of above ground facilities (Demir et al. 2014; Regenspurg et al. 2015; Scheiber et al. 2019; Westphal et al. 2019). These problems are currently countered by either regular clean-out operations of the boreholes or addition of acid or chemical inhibitors to the fluids.

Despite the extensive research on fluid chemistry and reactions of geothermal fluids during the past years, organic components were rarely included in the analyses and generally not considered in geothermal modeling. Implementing organic compound analyses in addition to the inorganic components, might greatly improve the understanding of the fluid-chemical properties. Specifically, carboxylic acids are known to act as strong complexing ligands for metals (Kharaka and Hanor 2003; Seewald 2001; Surdam et al. 1984). Organic geochemistry could be used as complementary tool to understand fluid dynamics and circulation within a reservoir as it was done and discussed for the Los Humeros geothermal field, Mexico, in Sánchez-Avila et al. (2021). Furthermore, organic compounds may serve as readily available nutrients for microorganisms. Reported effects of microbial activity in geothermal power plants are microbially induced corrosion of the casing due to metabolic byproducts (biofueling), formation of scales due to changes in the fluid chemistry (Inagaki et al. 2003; Westphal et al. 2019), and rapid growth of microbial communities forming biofilms, leading to decreasing flow rates and injection problems (Brehme et al. 2020).

The aim of this review is to present an overview of available data about dissolved organic compounds in geothermal fluids and discuss the origin, fate, and potential impact of these compounds on the overall fluid chemistry and performance of geothermal energy production. A general overview of organic compounds in deep subsurface fluids will be given in section [Types, origin, and occurrence of organic compounds in deep subsurface waters](#), while the main part of the review is focused on geothermal fluids that are used for energy production.

Types, origin, and occurrence of organic compounds in deep subsurface waters

Simplest organic compounds, just composed of carbon and hydrogen, are called hydrocarbons. They can be categorized into two types: aliphatic and aromatic hydrocarbons. The structure of aliphatic hydrocarbons is based on chains of C atoms, which are called alkanes if the atoms are joined together by a single electron bond and alkenes if one or more pairs of adjacent C atoms are joined together by a double bond (C=C) (Killops and Killops 2005). Alkanes can be further divided into compounds with an acyclic or cyclic structure. Acyclic alkanes are called *n*-alkanes when the carbon atoms form a straight chain (*n*-butane, Fig. 1), and branched alkanes when the

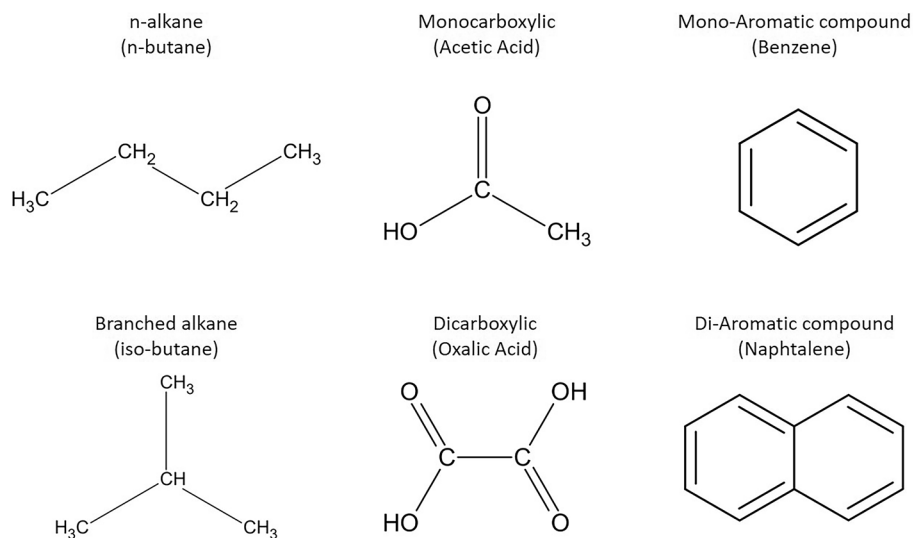


Fig. 1 Structural formula of various organic compounds representing *n*-alkanes and branched alkanes, monocarboxylic acids with one -COOH functional group and oxalic acid representing dicarboxylic acids with two functional groups, mono-aromatic and di-aromatic compounds

carbon atoms form more complex structures (*i*-butane, Fig. 1). The simplest aromatic hydrocarbon is benzene (C₆H₆), which consists of a ring of six C atoms with one hydrogen atom attached to each C atom. Other than cyclic alkanes, aromatic hydrocarbons are characterized by enhanced stability due to delocalized double bonds. Other atoms (heteroatoms) such as O, N and S can be incorporated in both aliphatic and aromatic hydrocarbons, oftentimes as functional groups (e.g., -OH, -NH₂, -SH). Furthermore, aromatic rings can be fused into polyaromatic structures (Fig. 1).

Dissolved organic carbon (DOC) describes the fraction of carbon from organic compounds being dissolved in water, which means passing through a 0.45- μ m filter. While DOC only refers to the mass of the carbon within the dissolved organic molecules, the term dissolved organic matter (DOM) refers to the bulk of organic molecules, including other atoms such as nitrogen, oxygen, sulfur and hydrogen. Figure 2 shows various size fractions belonging to DOM. The amount of DOC in shallow groundwater systems usually ranges from 0.2 to 15 mg CL⁻¹ with a median amount of 0.7 mg CL⁻¹ and derives either from organic matter transported from the surface (e.g., soil) or organic matter from sediments and rocks that was accumulated during their deposition (Leenheer et al. 1974; Thurman 1985). However, the DOC content of subsurface waters depends significantly on the regional settings, e.g., DOC concentration comprised 5–10 mg CL⁻¹ in groundwater associated with coals, 2–5 mg CL⁻¹ in oil shale waters (Thurman 1985), and up to 4900 mg CL⁻¹ in oil-field waters (Carothers and Kharaka 1978). Ground water samples of a variety of reservoir rocks showed a median DOC of 0.7 mg CL⁻¹ for sandstone, limestone, sand and gravel aquifers, and 0.5 mg CL⁻¹ in crystalline rocks (Leenheer et al. 1974). For DOC in deep subsurface groundwater systems, the buried sedimentary organic matter is of primary importance. Leaching processes can lead to mobilization of the sedimentary organic matter into the groundwater where it can be further processed in microbially active zones,

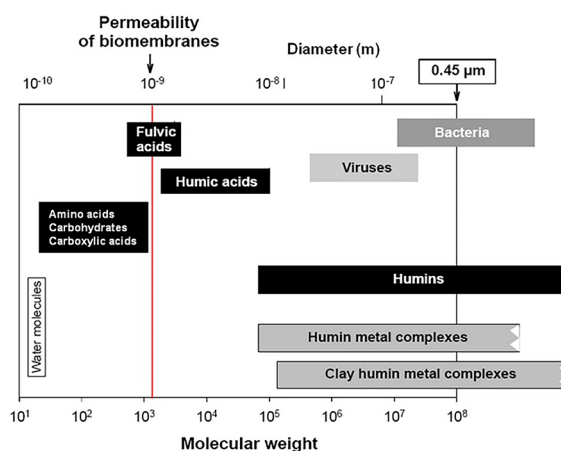


Fig. 2 Size fractions of different types of organic carbon. Modified by Vetter (2012) after Thurman (1985)

resulting in various metabolic byproducts contributing to the DOC (Filip and Smed-Hildmann 1992).

In depths and environments with increasing temperature, the process of thermal degradation of sedimentary organic matter of the host rock gains more importance to the release of DOC into the groundwater (Seewald 2001; You and Gieskes 2001).

Organic compounds can also be synthesized in biotic or abiotic reactions. Biotic processes involve the synthesis of organic compounds with relation to microorganisms, such as bacteria, algae, archaea, and fungi as part of their metabolism (Konn et al. 2011; McCollom and Seewald 2007; Poturay and Kompanichenko 2019; Simoneit et al. 2009). Abiotic processes can be further differentiated by the involvement of organic or inorganic precursors. Organic compounds may be synthesized from H_2 and CO_2 in high pressure and temperature systems due to fluid–rock interactions, in absence of complex organic precursors or biological activity (Reeves and Fiebig 2020). Organic compounds are of thermogenic origin if the organic precursors were thermally altered or degraded (Killops and Killops 2005).

According to Sánchez-Avila et al. (2021), aromatic compounds have been recognized to be predominant in hydrothermal environments. Several studies reported that hydrothermal conditions favor the formation of low molecular weight aromatic species such as mono- and poly-aromatic compounds like benzene and methylcoronene (McCollom et al. 2001; Simoneit 1993; Simoneit et al. 2004; Tassi et al. 2015).

It was also shown that short chain aliphatic acids can be released in great amounts from organic matter-rich deposits during maturation (Carothers and Kharaka 1978; Glombitza et al. 2009). Short chain aliphatic acids are water-soluble compounds consisting of 1–5 C atoms and the functional group of carboxylic acids ($-COOH$). The concentrations of monocarboxylic acid anions in oil-field waters are well described in many studies and are reported to be much higher than in groundwater. Acetate (CH_3COO^-) is described as the most abundant species and concentrations may reach values of up to $10,000 \text{ mg L}^{-1}$ (Kharaka et al. 2000; MacGowan and Surdam 1990). The abundance of other monocarboxylic acid anions generally decreases with increasing number of carbon atoms (acetate > propionate > butyrate > valerate) (Carothers and Kharaka 1978;

Fisher and Boles 1990; Kharaka et al. 1987). Formate (CHOO^-) does not seem to follow this trend with a reported maximum concentration of 174 mg L^{-1} in oil-field waters (Kharaka et al. 1985a; MacGowan and Surdam 1988; Surdam et al. 1984). Concentrations of dicarboxylic acid anions range from 0 to 2540 mg L^{-1} in formation waters from sedimentary basins (Kharaka et al. 2000; MacGowan and Surdam 1988). However, the data are much more limited compared to monocarboxylic acid anions. In oil-field waters concentrations of both, mono- and dicarboxylic acid anions, are mainly controlled by the subsurface temperature (Carothers and Kharaka 1978).

Three temperature zones were first introduced in Kharaka et al. (1988) (Fig. 3). Zone 1 with maximum temperature of 80°C is characterized by acid anion concentrations of

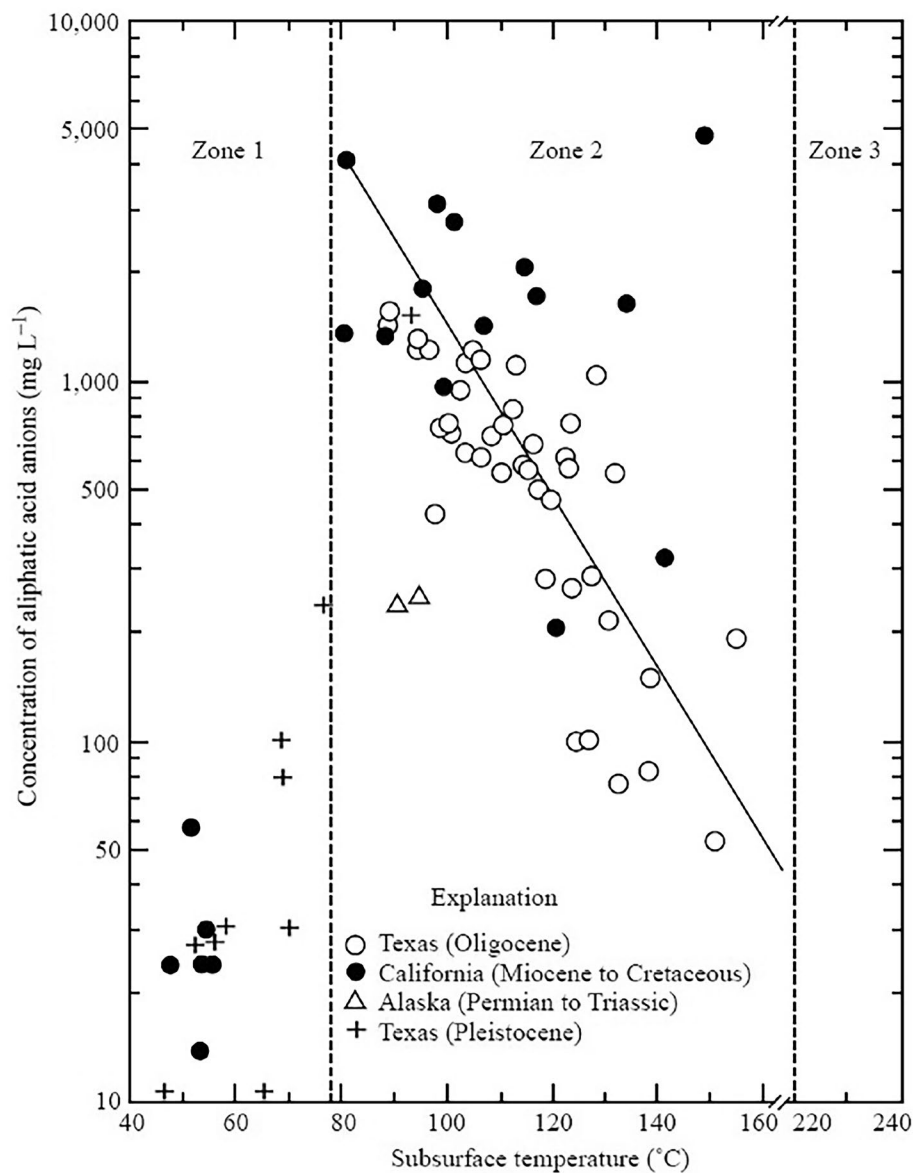


Fig. 3 Concentrations of aliphatic acid anions ($\text{C}_2\text{--C}_5$) in formation waters from three sedimentary basins. Highest concentrations are at 80°C and thereafter decrease with increasing temperatures (source Kharaka et al. (1988) and Kharaka and Hanor (2003))

less than 500 mg L^{-1} . In this zone, acetate concentrations are generally low, while propionate predominates. In Zone 2 from $80\text{--}200^\circ\text{C}$, the concentrations were reported to be much higher and decreasing with increasing temperature. Total organic acid anions consist of about 90% acetate and 5% propionate (Carothers and Kharaka 1978; Lundegard and Kharaka 1994). The boundary of Zone 3 was placed at 220°C , where no measurable organic acid anions were present. This Zone was based on extrapolation from data of Zone 2 (Kharaka et al. 1985b). The low acetate concentrations and predominant occurrence of propionate in Zone 1 were attributed to microbial degradation of acetate, while the decrease or absence of organic acid anions with increasing temperature in Zone 2 and 3 were attributed to thermal decarboxylation (Carothers and Kharaka 1978) (Eq. 1).



The degree of decarboxylation was also interpreted to correlate with the age of the reservoir formation. The highest concentrations in Zone 2 were present in the youngest (7.5–19 million years) and shallowest reservoir rocks from the Miocene with temperatures between $80\text{--}120^\circ\text{C}$, while they were decreasing with increasing subsurface temperature and age of the reservoir rocks (Kharaka et al. 2000). However, organic acid concentrations of the Palo Duro Basin, Texas, appeared to be associated with longer groundwater residence time (Means and Hubbard 1987). Thermal decarboxylation starts at temperatures above 100°C and is accounted to be the main driver of the conversion from organic acid anions to CO_2 and hydrocarbon gases (Carothers and Kharaka 1978; Kharaka et al. 2000). Several studies showed that the $\delta^{13}\text{C}$ from CO_2 and CH_4 in natural gas, and diagenetic ankerite and calcerite from the Gulf Coast and California basins, result largely from the thermal degradation of organic matter (Boles 1978; Carothers and Kharaka 1980; Lundegard and Kharaka 1994; Lundegard and Land 1985).

In deep subsurface sediments with temperatures below 120°C , where microbial life is still possible (e.g., extreme thermophiles and hyperthermophiles), organic material may be metabolized both aerobically and anaerobically (Lovley and Chapelle 1995). Aerobic bacteria readily degrade short chain aliphatic acids by oxidizing O_2 . Anaerobically, organic matter can be metabolized by the reduction of iron, manganese, sulfate and H_2 . Novak and Ramesh (1975) describe short chain aliphatic acids to be products of a multi-step process in which complex organic matter is degraded by facultative anaerobic bacteria under reducing conditions. Because most anaerobic bacteria are very limited in the types of organic compounds they can oxidize, complex organic compounds are first metabolized by fermentative microorganisms (Lovley and Chapelle 1995). Studies from Lovley and Klug (1986), Lovley and Phillips (1989), Sørensen et al. (1981) indicate that in sedimentary environments the predominant fermentation products are acetate and hydrogen, however, other short chain aliphatic acids such as propionate and butyrate are also produced. Depending on the prevailing environmental conditions, microbial activity may have a great effect on the molecular composition of DOM. The occurrence of microorganisms in geothermal systems and comparable environments is described more in detail in (Bregnard et al. 2022).

Generally, the abundance and distribution of short chain aliphatic acids in groundwater reflect the rates of several major processes: (a) their genesis from sedimentary organic matter and expulsion into the formation fluid; (b) thermal decarboxylation; (c)

bacterial transformation and degradation; and (d) reservoir flushing (Means and Hubbard 1987).

So far, most studies on organic geochemistry in deep fluids are focused on a variety of deep subsurface environments, such as oil field waters. Only few studies were conducted to investigate fluids from geothermal power plants. Water samples from geothermal fluids and other deep fluids have been analyzed for their DOC concentration and content. This work is summarized in Table 1. This review will specifically focus on the sites from the North German-, Molasse-, Styrian-, Baltic Sea-, and Vienna Basin, Upper Rhine Valley, Russian geothermal fields, and the Los Humeros geothermal field, since these sites are used for geothermal energy production.

Methods used to characterize DOM

Concentrations and composition of organic compounds in water samples can be determined by a multitude of analytical methods. Here, the analytical methods are shortly described that have been applied to characterize the DOM in these fluids from geothermal plants that will be presented in detail in the following chapters. Quantification and characterization of DOC is done via liquid chromatography organic carbon detection (LC-OCD) (Huber and Frimmel 1996). The molecules belonging to DOM can be differentiated by their molecular masses with size exclusion chromatography, where an increasing retention time in the chromatographic column indicates decreasing molecular masses (Pelekani et al. 1999). The resulting fractions are: biopolymers (bio), humic substances (Hs), building blocks (BB), low molecular weight organic acids (LMWOA), low molecular weight neutrals (LMWN), and hydrophobic organic carbon (HOC) (Huber et al. 2011) (Table 2). These DOC fractions are given as percentage of the total DOC. Ion chromatography (IC) is used to determine the main organic acid anions (formate, acetate, propionate, butyrate, valerate, oxalate).

Gas chromatography–mass spectrometry (GC–MS) is applied to organic extracts of both, solid and fluids samples. Here, differentiation of the organic matter into percentage of *n*-alkanes, aromatics, S-bearing and O-bearing compounds was done (Kompanichenko et al. 2016; Poturay 2017; Sánchez-Avila et al. 2021).

Types of geothermal systems considered in this review

One approach to classify geothermal systems is with respect to their temperature, enthalpy, and physical state of the fluid (Table 3) (Bodvarsson 1961; Saemundsson et al. 2009). Additionally, they can be also classified based on their geological setting. Following the characterization in Saemundsson et al. (2009), the geothermal systems used for energy production presented in this review are: low- to medium-temperature sedimentary systems and high-temperature volcanic systems.

Sedimentary systems are found in many of the major sedimentary basins such as the Molasse Basin (Germany), the Paris Basin (France), the Great Artesian Basin (Australia), and the Turfan Basin (China). They are characterized by permeable sedimentary layers at depths above 1 km, however their origin and heat flow can differ widely, as well as the salinity of the reservoir fluids. Volcanic systems are situated inside or close to calderas and the heat source derives from intrusions or magma. Here, the fluid flow is mostly controlled by fractures and fault zones.

Table 1 Overview on DOC and LMWOA concentrations, and DOC composition in water samples from different geothermal regions of the world

Site	Temperature (°C)	Depth (m)	Geol. Formation	DOC (mg C L ⁻¹)	LMWOA (mg L ⁻¹)	Other
South African Mines Kieft et al. (2018)						
Beatrix	34–38***	1339	Witwatersrand quartzite	0.2–1.5	0.04–0.44	Aliphatics, carboxyls, aromatics
Driefonteine	26.8***	1046	Transvaal dolomite	0.3–1.02	0.01–0.55	
Kloof	54.5***	3276	Ventersdorp metavolcanics	4.92	0.68–0.77	
Tau Tona	49–51***	3048	Witwatersrand quartzite	0.22–0.73	0.01–0.19	
Star Diamonds	31***	640	Karoo sandstone	0.25	0.02–0.07	
Joel	39.9***	1300	Witwatersrand quartzite	0.18	0.04–0.07	
Masimong	40.7***	1900	Witwatersrand quartzite	0.54	0.02–0.07	
Koffiefontein	28.9***	578	Archean gneiss	n.d	< 0.11	
Finsch	28.9***	1056	Transvaal dolomite	n.d	0.3–0.31	
Pannonian Basin						
Kovacs et al. (2012)	41–83**	1000–2100	Late Miocene and Pliocene sandstones	8.5–139 ^a		Carboxyls, aromatics aliphatics humic content: 2.9–9.5 mg/L
Varsányi et al. (2002)	38–111*	490–2200	Quaternary–Upper Miocene sediments	2.5–28 ^a	n.d–38.5	Humic content: 0.1–15.7 mg/L aromatics: 0.11–24.94 µg/L phenols
Varsányi et al. (2002)	17–56*	240–816	Quaternary–Pleistocene sediments	6.8–84 ^a		Humic content: 9.71–30.52 mg/L aromatics: n.d–20 µg/L phenols
Varsányi et al. (2002)	50–132*	701–2181	Pleistocene–Upper Miocene sediments	4.8–550 ^a	n.d–923	Humic content: 1.2–50.1 mg/L aromatics: n.d–17.29 µg/L
Kárpáti et al. (1999)	12–99*	30–2500	Quaternary–Upper Miocene sediments	n.d–46		Humic content: n.d–12.5 aromatics, phenols, fatty acids <i>n</i> -alkanes
North German Basin						
NG1 Leins et al. (2022)	34***	850	Upper Keuper sandstone	4.9	n.d	
NG2 Leins et al. (2022)	64***	1620	Lower Dogger sandstone	2.5–7.7	1.8–2	
NG3 Leins et al. (2022)	98**	2450	Upper Keuper sandstone	19.5–25.9	44.8–49.3	
Groß Schönebeck (NG4) Feldbusch (2015)	150*	4400	Permo-Carboniferous sediments and volcanic rocks	25	29.77	

Table 1 (continued)

Site	Temperature (°C)	Depth (m)	Geol. Formation	DOC (mg C L ⁻¹)	LMWOA (mg L ⁻¹)	Other
Molasse Basin Vetter (2012); Leins et al. (2022)						
M2-M8	65–135*/**	2250–4083	Jurassic carbonate (Malmian)	0.35–30.1	n.d–16.9	
Styrian Basin Westphal et al. (2019)						
Bad Blumau (S1), Austria	107**	2800	Palaeozoic carbonate	14.5		
Vienna Basin Leins et al. (2022)						
V1	53*	900	Middle Miocene conglomerate	0.22–1.51	n.d	
Baltic Sea Basin Brehme et al. (2019)						
Klaipeda (B1), Lithuania	38*	1100	Devonian sandstone	1.6–2.4		
Russian geothermal fields						
Mutnovskii Kompanichenko et al. (2016)	175**	1600–1800	Quarternary–Oligocene sediments and volcanic rocks			Aromatics, O-bearing, Cl-bearing, S-bearing hydrocarbons
Annenskii Poturay (2017)	99**	44–202	Cretaceous volcanic and tuff sedimentary rocks			<i>n</i> -Alkanes, esters, alcohols, carboxylic acids, terpenes, steroids
Los Humeros geothermal field, Mexico						
Sánchez-Avila et al. (2021)	292–348**	1800–2800	Neogene–Quarternary volcanic rocks			<i>n</i> -Alkanes, aromatics, S-bearing, O-bearing hydrocarbons
Upper Rhine Valley Sanjuan et al. (2016)						
RV1–RV5	66–200*	1547–5000	Triassic–Carboniferous sediments and granite	0.7–35.2		
Canadian Shield Sherwood Lollar et al. (2021)						
Kidd Creek	23–27***	2400	Precambrian metasedimentary, metavolcanic rocks	29–60	64–94	
Thompson	21.9–22.7***	1200	Precambrian meta-sedimentary, metavolcanic, ultramafic rocks	0.61–8.7	0.1–8	
Lost City Hydrothermal Fields (Mid-Atlantic Ridge)						
Lang et al. (2010)	31–91*	Seafloor	Mantle rocks	0.7–1.2	n.d–6.9	Alkanes, cycloalkanes, aromatics, carboxyls
East African Rift Valley Hot Springs Butturini et al. (2020)						
Ol Njorowa	>50**	–	Pleistocene basalts, trachytes, pyroclastics	1.67		Aromatics, carboxyls aliphatics

Table 1 (continued)

Site	Temperature (°C)	Depth (m)	Geol. Formation	DOC (mg C L ⁻¹)	LMWOA (mg L ⁻¹)	Other
Lake Elementaita	36.6**	–	Pleistocene basalts, trachytes, pyroclastics	0.97		Aromatics, carboxyls aliphatics
Thermal Water Springs						
Ourense, Spain González-Barreiro et al. (2009)	45.6–66.3**	–	Granitic rock			amines/amides, esters, acids, alcohols, aliphatic/alicyclic/aromatics, Phenols
Calabria, Italy Di Gioia et al. (2006)	–	–				Phenols, fatty acids, long-chain saturated and unsaturated alcohols, long-chain carboxylic acids and alcohols, <i>n</i> -alkanes

n.d.: not detectable; *subsurface, ** surface, *** not specified; ^a TOC

Table 2 Description of LC-OCD fractions. Modified from Huber et al. (2011), Penru et al. (2013), and Zhu et al. (2015)

Fraction	Properties	Description
Hydrophobic organic carbon	Hydrophobic	Lipids (fats) released from bacteria and algae
Biopolymers	Not UV-absorbable, hydrophilic	Polysaccharides and proteins
Humic substances	Highly UV-absorbable, hydrophobic	Side products of bacterial decay
Building blocks	UV-absorbable	Breakdown products of humic substances
Low molecular weight organic acids	Negatively charged	Aliphatic acids
Low molecular weight neutrals	Weakly or uncharged hydrophilic, amphiphilic	Alcohols, aldehydes, ketones, amino acids

Overview on DOM content and composition in fluids from geothermal power plants

Data on DOM from both, low-to-medium enthalpy geothermal sites (Germany, Austria, Lithuania, France, and Russia), and high-enthalpy geothermal sites (Mutnovskii, Russia and Los Humeros, Mexico) were available for this study. In total, data of 143 fluid samples from 22 geothermal sites were collected. The locations of the low-enthalpy geothermal sites in central Europe are shown in Fig. 4. Due to confidentiality agreements some site locations cannot be mentioned by name and are instead represented with a site ID. Mainly, sites from the Molasse Basin (M2 to M8) and sites from the North German Basin (NG1 to NG4) make up the data and present DOC and short chain aliphatic acid anion concentrations. They were compiled from Vetter (2012), Feldbusch (2015), and (Leins et al. 2022). Upper Rhine Valley (RV1 to RV5) data originate from Sanjuan et al. (2016), Bad Blumau (S1) data from Westphal et al. (2019), some of the Klaipeda (B1) values from

Table 3 Classification of geothermal systems with regard to temperature enthalpy and physical state after Saemundsson et al. (2009); Bodvarsson (1961)

Temperature	Enthalpy	State
Low-temperature (LT) systems with reservoir temperature at 1 km depth below 150°C. Often characterized by hot and boiling springs.	Low-enthalpy geothermal systems with reservoir fluid enthalpies less than 800 kJ kg^{-1} , corresponding to temperatures less than 190°C.	Liquid-dominated geothermal reservoirs with the water temperature at, or below, the boiling point at the prevailing pressure and the water phase controls the pressure in the reservoir. Some steam may be present.
Medium-temperature (MT) systems with reservoir temperature at 1 km depth between 150–200°C.		
High-temperature (HT) systems with reservoir temperature at 1 km depth above 200°C. Characterized by fumaroles, steam vents, mud pools and highly altered ground.	High-enthalpy geothermal systems with reservoir fluid enthalpies greater than 800 kJ kg^{-1} .	Two-phase geothermal reservoirs where steam and water co-exist and the temperature and pressure follow the boiling point curve. Vapor-dominated reservoirs where temperature is at, or above, boiling at the prevailing pressure and the steam phase controls the pressure in the reservoir. Some liquid water may be present.

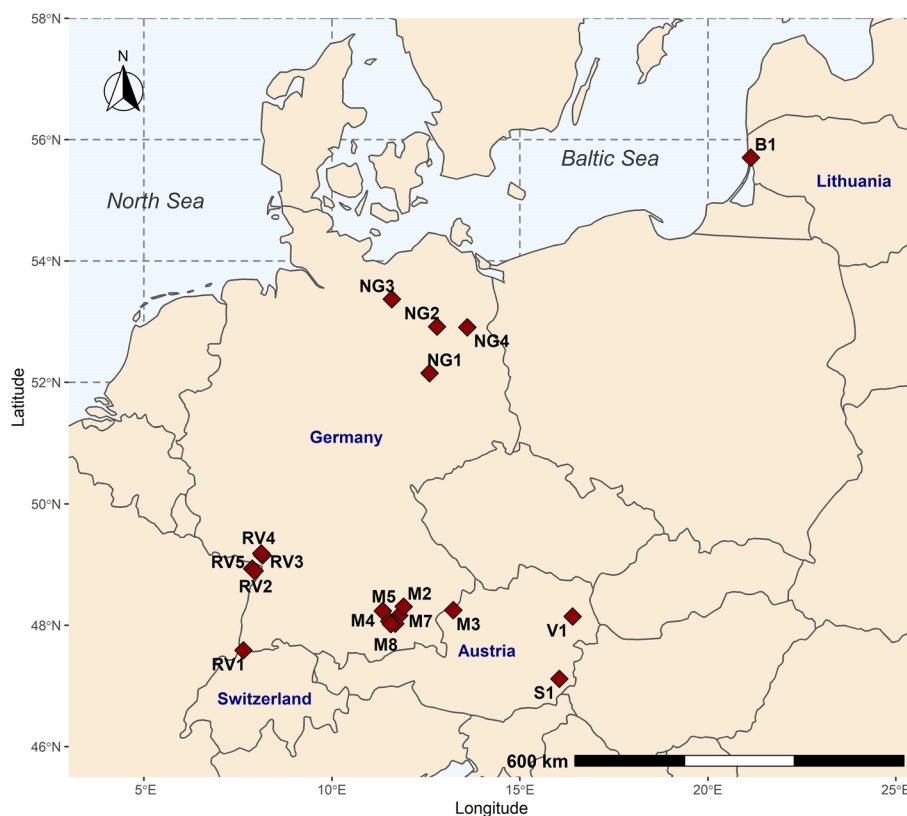


Fig. 4 Location of the geothermal sites in central Europe from which data on organic compounds are available

Brehme et al. (2019) and remaining data were compiled from analyses of various fluid samples (Leins et al. 2022). Fluids from high-enthalpy sites have been analyzed for their abundance of organic compound classes, such as *n*-alkanes, aromatics, and carboxylic acids (Kompanichenko et al. 2016; Poturay 2017; Sánchez-Avila et al. 2021).

It is important to note that the construction of a geothermal power plant (drilling, hydraulic stimulation, clean-out operations) can greatly affect the chemical composition of the subsurface reservoir by introducing oxygen, acids, drilling mud and other components into the reservoir (Kloppmann et al. 2001; Regenspurg et al. 2010, 2018). In operating geothermal power plants, where mineral scaling is an issue, organic scaling inhibitors are added to the produced fluids, which contributes to the measured DOM (e.g., Westphal et al. (2019)). Therefore, DOM characterization of those fluids must be viewed with caution when it comes to the original/pristine fluid composition. For example, contamination due to drilling mud is only given in the first years of operation (Vetter 2012). With continuous fluid production, the drilling mud in the borehole dilutes and is probably removed from the system.

Geothermal fluids in the North German Basin

The North German Basin (NGB) is the largest sub-basin of the Central European Basin (CEB) (Gast et al. 1998) and extends from Poland through Germany, Denmark, the

Netherlands, the southern North Sea, to eastern England and the Atlantic Shelf (Lüders et al. 2010). The deposition of Rotliegend volcanic rocks between late Carboniferous and early Permian started the formation of the NGB (Tesmer et al. 2007), followed by a long-lasting subsidence (> 250 Ma) (Scheck et al. 1999). Aeolian sandstones, fluvial fans, and playa deposits formed a clastic sequence (Lower Permian, Rotliegend) covering the Permo-Carboniferous volcanic rocks (Rieke et al. 2001). During the Upper Permian, carbonates and evaporites were deposited due to repeated marine transgressions (Tesmer et al. 2007). The deposition of sediments and the E–W extension of the basin during the Triassic and late Jurassic led to the mobilization of the underling Zechstein evaporites (Vosteen et al. 2004). Several stages of sedimentation occurring in the Mesozoic were described by Tesmer et al. (2007). Starting with terrestrial red-bed sequences (Lower Triassic: Bunter), followed by depositions of shallow marine facies (Middle Triassic: Muschelkalk), thereafter by mainly terrestrial facies of sandstones interbedded by carbonate, anhydrite, and halite sequences (Upper Triassic: Keuper), and ending in a mainly marine environment (Jurassic and Cretaceous). Further movements of those salt layers contributed to the deformation of the basin leading into the formation of sub-basins and troughs (Tesmer et al. 2007).

Formation waters of the NGB generally contain high concentrations of dissolved solids, exceeding the values of surface, marine or meteoric water (Kloppmann et al. 2001; Moeller et al. 2008). They contain mainly chloride, followed by sodium and calcium, and minor amounts of magnesium, and potassium (Lüders et al. 2010). In the NGB, DOM data were reported for four sites. NG1 and NG3 both target the formations of the Upper Keuper (Triassic), however in different depths of 850 m and 2456 m, respectively (Franz et al. 2018; Seibt et al. 2005). NG2 targets the Lower Dogger (Jurassic) (Göthel 2014) and NG4 targets the Lower Rotliegend (Permo-Carboniferous) (Regenspurg et al. 2016). Compared to the other sites, NG4 does not target a single formation but rather an intersection of sedimentary and volcanic rocks including three types of reservoir units. The upper sandstone (Dethlingen Formation), lower sandstone (Havel Formation), and Permo-Carboniferous volcanic rocks with a respective fluid contribution of 14%, 52%, and 30% as shown from flowmeter measurements in 2007 (Henninges et al. 2012).

According to investigations by Beer and Manhenke (2001), Neumann (1975), Voigt (1975) deep aquifer complexes (DAC) in the east of the NGB can be subdivided in four deeper complexes (DAC 1–4), which are separated by low permeability complexes (LPC). However, hydraulic connections between the deep saline aquifers and freshwater bodies exist locally along fault zones and along Pleistocene channels at places where LPCs were eroded or not deposited. Following the subdivision of those four distinct aquifer systems, NG1, NG2 and NG3 produce fluids from the DAC 1 complex, which extends from the Lower Tertiary to the Upper Triassic. NG4 produced fluids are contributing to the DAC4 complex, which is characterized by the Lower Rotliegend. Tesmer et al. (2007) and Moeller et al. (2008) stated that none of the formation waters from Mesozoic aquifers can be classified as original formation water due to intensive fluid flow between aquifers.

The depth of the production wells and the temperature display a good positive correlation with a minimum depth of 850 m and temperature of 34 °C at NG1 and maximum depth of 4400 m and temperature of 150 °C at NG4 (Table 4). Mean DOC

Table 4 Organic and inorganic fluid chemistry of NGB sites (mg L^{-1})

Element/ion	NG1	NG2	NG3	NG4
Depth (m)	850	1620	2455	4400
Temperature ($^{\circ}\text{C}$)	34	64	98	150
K	379	446	782	2560
Na	690,000	74,700	80,010	33,600
Ca	1360	1540	8409	45,400
Mg	914	1070	1410	233
Sr	39.5	n.m	440	1290
Fe	4.8	31	60	47.1
Li	0.65	n.m	8.3	212
Mn	0.14	1.2	10	131
TDS	187,000	199,000	221,000	265,000
Cl	108,000	116,800	137,000	138,384
Br	62	111	390	215
SO_4	3360	3830	470	94.4
HCO_3	253	247	40	n.m
NH_4	27.2	n.m	n.m	14.2
DOC	4.9	5.16	22.8	23.4
Formate				
(mg L^{-1})	n.d	0.7	0.3	24.7
(mg C L^{-1})	n.d	0.19	0.08	6.6
Acetate				
(mg L^{-1})	n.d	0.9	44.95	1.2
(mg C L^{-1})	n.d	0.37	18.29	0.49
Propionate				
(mg L^{-1})	n.d	n.d	1.4	n.d
(mg C L^{-1})	n.d	n.d	0.69	n.d
\sum LMWOA				
(mg L^{-1})		1.8	46.65	29.77
(mg C L^{-1})		0.56	19.09	8.11

DOC, formate, acetate, and propionate (mg C L^{-1}) represent the mean values of the production well from organic compound data compiled from Leins et al. (2022). For NG4 the last sample from the pump test in April 2012 was taken (Feldbusch 2015). Inorganic data were compiled from Steintherme.de (2021) (NG1), Seibt et al. (2008) (NG2), Seibt et al. (2000, 2005) (NG3) and Regensburg et al. (2016) (NG4)

n.m: not measured, n.d: not detected

LMWOA: low molecular weight organic acids

values range from 4.9 to 23.4 mg C L^{-1} (Fig. 5). Formate concentrations range from 0.08 to 6.6 mg C L^{-1} . At NG4 they are significantly higher than in the other NGB sites. The other sites report very low-to-none traceable concentrations. Acetate values range from 0.37 to 18.29 mg C L^{-1} . Highest acetate concentrations were determined in samples from NG3, all other sites have low concentrations or even not detectable concentrations of acetate. Propionate was only detected in low concentrations (0.69 mg C L^{-1}) in fluids of NG3.

Data from NG4 originate from a long-time circulation test done in April 2012 (Feldbusch 2015). At that time, water was produced for 150 h from the production well and directly injected into the injection well. The samples were collected at the wellhead of the production well. Water samples had constantly low acetate concentrations, while

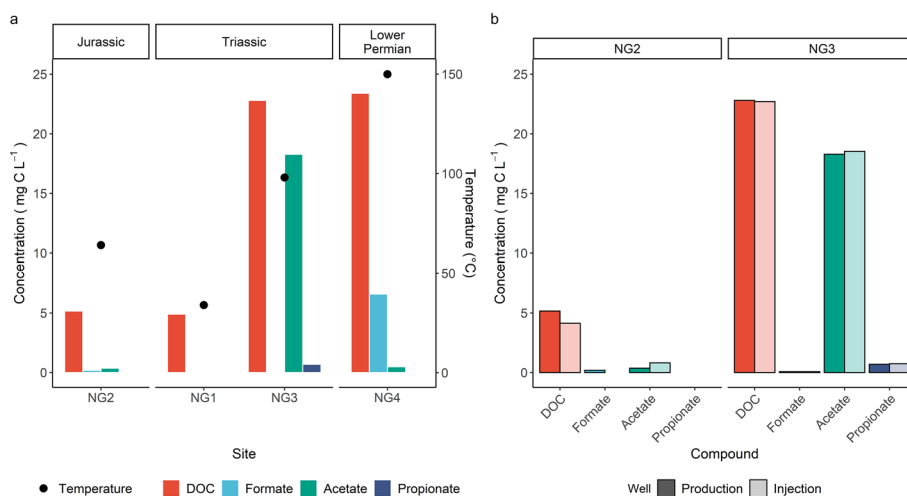


Fig. 5 **a** Mean concentrations of DOC, formate, acetate, propionate (mg CL⁻¹) and the temperature for each reported site of the North German Basin. The sites on the x-axis are arranged primarily after reservoir age (youngest to oldest from left to right) and secondarily after the well depth (shallowest to deepest from left to right) within the grouped rectangles. **b** Mean concentrations compared between production (dark fill) and injection (clear fill) well. Missing data represent either data below detection limit or not reported data

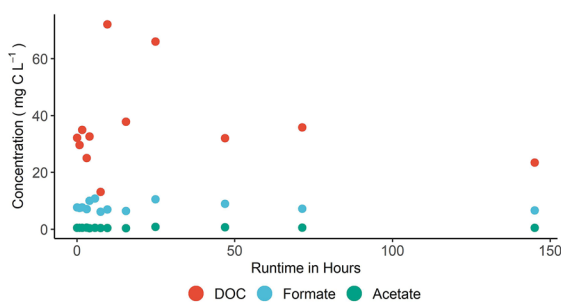


Fig. 6 Organic compound concentrations in fluid samples taken from the production well during long-time circulation test at NG4 in April 2012

formate varied between 6–11 mg CL⁻¹ in the first hours of the test (Fig. 6). At the end of the experiment the formate concentration was at 6.6 mg CL⁻¹. As with formate concentrations, also DOC concentrations varied strongly in the beginning of the test (10–70 mg CL⁻¹) and were stabilized at approximately 23.4 mg CL⁻¹ in the end of the experiment. Assuming that the fluid produced at the end of the long-time circulation test was the most undisturbed and most comparable to natural fluid, the concentrations of the last sample was taken as representatives for NG4.

Although, NG1 and NG3 were sampled from the same formation, organic compound concentrations differ significantly. NG1 has a DOC of 4.9 mg CL⁻¹ and no detected organic acid anions, while NG3 has a DOC of 22.8 mg CL⁻¹ including an acetate content of 18.29 mg CL⁻¹. This might be explained by even more locally attributed water–rock interactions affecting the organic composition or simply by water contamination due to well operations. None of the Mesozoic aquifer fluids in NG1, NG2 and NG3 can be classified as the original formation water due to intensive fluid flow between aquifers (Moe-ller et al. 2008; Tesmer et al. 2007). Therefore, detected organic compounds might not

be associated with the reservoir rocks of NG1 to NG3. Data of inorganic compounds from the literature are presented in Table 4, showing a general increase in total dissolved solids (TDS) and Cl from NG1 to NG4. Seemingly, DOC concentrations are higher in deeper and older reservoirs and are correlated to high concentrations of total dissolved solids and uncorrelated to increasing temperatures up to 150 °C.

Throughout all data, the difference in concentrations of the reported organic compounds is very low between samples from production and injection side. The highest difference was observed for acetate in NG2, with an increase of 0.44 mg CL⁻¹ from the production (0.37 mg CL⁻¹) to the injection side (0.81 mg CL⁻¹).

Geothermal fluids in the Molasse Basin

Located north of the alps in southern Germany, the Molasse Basin (MB) is a foreland basin that extends from the Lake Geneva area in the west to Lower Austria in the east (Bachmann et al. 1987; Mayrhofer et al. 2014). The basin thickens from north to south, reaching up to 5000 m at the front of the Alps. It is filled predominantly with clastic sediments of Tertiary age underlain by 500–1000 m of Mesozoic shelf sediments, local Permo-Carboniferous troughs, and the Variscan basement (Bachmann et al. 1987).

The main deep subsurface aquifer used for geothermal exploitation lies within the upper Malm formation (Mayrhofer et al. 2014). The Malm was formed during the Late Jurassic, when a large sea level rise flooded the south German region followed by deposition of up to 600 m of limestone and marls. By the end of the Jurassic, the carbonate sediments were partly exposed to the land surface due to a sea level fall, leading to karstification (Mayrhofer et al. 2014). The upper Malm formation is characterized as a karstified carbonate deep groundwater aquifer, which dips to the south.

The water composition differs from the margin regions of the basin to the center of the basin as percolating meteoric water from the MB borders (Swabian and Franconian Albs, and the Bohemian Massif) recharges the groundwater (Andrews et al. 1987; Goldbrunner 2000; Stichler et al. 1987). Hence, the age of the fluids is reported to be between 10,000 and 50,000 years (Andrews et al. 1987; Goldbrunner 1997). Generally, the concentration of total dissolved solids does not exceed 1 g L⁻¹, however sometimes it can reach up to 5 g L⁻¹ due to locally restricted areas where mixing with Tertiary aquifers can occur (Wolfgramm and Seibt 2008). The fluids of the MB are described as Ca–(Na)–(Mg)–HCO₃–(Cl) type (Vetter 2012). A trend where Ca²⁺, Mg²⁺, and HCO₃⁻ concentrations decrease with increasing depth was reported, whereas Na⁺ and Cl⁻ increase (Wolfgramm and Seibt 2008).

The Molasse Basin is also known to contain numerous oil and gas fields (Bachmann et al. 1987). Main oil and gas reservoirs are associated with Cenomanian and Eocene shallow marine sandstones (Fig. 7), while minor deposits are found in Jurassic clastic rocks and algal limestones of the Upper Eocene. Main thermogenic hydrocarbon source rocks are also associated with deep marine Lower Oligocene pelitic rocks (Pytlak Ł et al. 2017; Sachsenhofer and Schulz 2006; Sachsenhofer et al. 2010). Although, the Malm aquifer is generally considered separated from aquifers of overlying stratigraphic units (Huber 1999), other studies suggested hydraulic connections between the Malm aquifer and oil-bearing rocks (Andrews et al. 1987; Goldbrunner 2000; Gross et al. 2015).

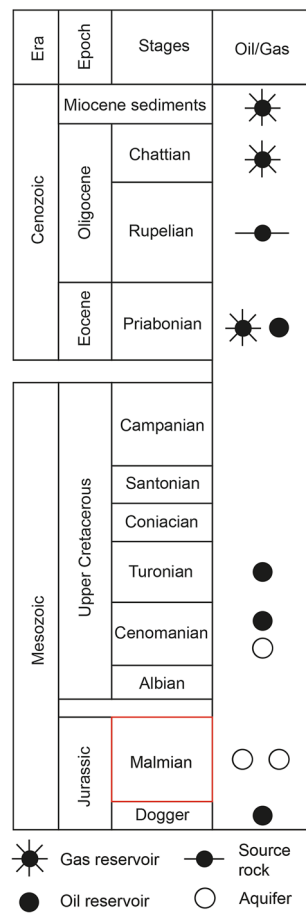


Fig. 7 Time stratigraphic table of the Austrian part of the Alpine Foreland Basin. The German part of the basin also includes the Barremian, Hauterivian, and part of the Berriasian stages of the Lower Cretaceous. The Malmian strata (outlined in red), is targeted for geothermal energy production in the MB. Source rock, oil and gas occurrences are indicated after Grunert et al. (2015); Nachtmann and Wagner (1987). Figure adapted from Pytlak et al. (2017)

Data on organic compounds in the MB were available for seven sites with M2 to M5 (Leins et al. 2022; Vetter 2012). Data for the sites M6 to M8 were only compiled from Leins et al. (2022). All sites from the MB target Malm aquifer, however at different depths (Table 5). The sites M2, M4 and M5 are located in the center of the MB around Munich, while M3 is located in the Austrian part of the MB (Vetter 2012). It is also reported that M3 has a specific feature of having significantly higher temperatures than M2 at almost the same target depth due to its artesian aquifer, and that M4 also incidentally produces oil (Vetter 2012). Furthermore, until 2012 this site was operated as doublet system with one production and one injection well. Since 2012 a third well was connected forming a triplet system with the two old wells as the production wells and the new third well as injection well. The doublet system is named M4, whereas the later triplet system is renamed M4.1. The sites M6, M7 and M8 are also located in the center of the MB.

To date, no literature was found that describe the application of chemical inhibitors in the geothermal plants M2 to M8. It is assumed that these plants also are operating under high pressure to counter the effects of degassing and scaling. The use and the effects of

Table 5 Average organic and inorganic fluid chemistry of MB sites (mg L^{-1} and mg CL^{-1}), DOC (mg CL^{-1}) from production side samples

Element/ion	M2	M3	M4	M4.1	M5	M6	M7	M8
No. of samples	2 (10)	2 (3)	4 (5)	5	2 (8)	1	1	2
Depth (m)	2250	2300	3443	3443	3446	3014	3882	4083
Temperature ($^{\circ}\text{C}$)	65	106	107	107	123	76	135	130
Water type	Na–Ca– HCO_3 –Cl	Na– HCO_3 –Cl	Na– HCO_3 –Cl	Na– HCO_3 –Cl	Na– HCO_3 –Cl	n.m	n.m	n.m
TDS	600	1300	900	n.m	< 1000	n.m	n.m	n.m
Cl	82.3 (71.5)	172 (164)	266.6 (273.8)	259.6	101.6 (109.2)	71.3	221	170
F	2.05 (2.19)	5.84	3.68	3.88	4.63 (4.74)	n.m	n.m	6.38
Br	n.m (0.29)	n.m	3.66 (3.68)	0.9	n.m (0.63)	n.m	n.m	2.37
SO_4	22.17 (9.36)	5.62	34.57 (36.19)	20.38	29.45 (26.68)	n.m	n.m	39.7
DOC	0.35 (0.55)	0.85 (0.77)	10.45	7.86	2.1 (2.54)	0.7	30.1	2.8
Formate								
(mg L^{-1})	< 0.1(0.1)	0.2 (0.15)	1.23 (1.15)	0.83	0.25 (0.31)	0.1	2.7	0.29
(mg CL^{-1})	(0.03)	0.05 (0.04)	0.33 (0.3)	0.22	0.07 (0.08)	0.03	0.72	0.08
Acetate								
(mg L^{-1})	n.d	0.55 (0.5)	12.58 (12.04)	10.32	2.44 (3.26)	0.3	11.6	5.01
(mg CL^{-1})	n.d	0.22 (0.20)	5.11 (4.89)	4.19	0.99 (1.33)	0.12	4.72	2.04
Propionate								
(mg L^{-1})	n.d	n.d	2.37 (2.37)	2.64	0.43 (0.6)	n.d	0.1	0.78
(mg CL^{-1})	n.d	n.d	1.17 (1.17)	1.3	0.21 (0.3)	n.d	0.05	0.38
Butyrate								
(mg L^{-1})	n.d	n.d	0.55 (0.56)	0.64	0.12 (0.13)	n.d	n.d	0.22
(mg CL^{-1})	n.d	n.d	0.3 (0.31)	0.35	0.06 (0.07)	n.d	n.d	0.12
Valerate								
(mg L^{-1})	n.d	n.d	0.18 (0.17)	0.18	n.d	n.d	n.d	n.d
(mg CL^{-1})	n.d	n.d	0.11 (0.1)	0.11	n.d	n.d	n.d	n.d
\sum LMWOA								
(mg L^{-1})	< 0.1(0.1)	0.75 (0.64)	16.91 (16.29)	14.61	3.24 (4.3)	0.4	14.4	6.3
(mg CL^{-1})	0.03	0.27 (0.24)	7.02 (6.77)	6.17	1.33 (1.78)	0.15	5.49	2.62

Data for M2, M3, M4, and M5 were compiled from Vetter (2012) and Leins et al. (2022). Values for M4.1, M6, M7, and M8 are from Leins et al. (2022). Values within brackets show the average concentrations when data from both Vetter (2012) and Leins et al. (2022) are included in the calculation

n.m: not measured, n.d: not detected

LMWOA: low molecular weight organic acids

inhibitors in the MB sites are currently investigated (Keim et al. 2020; Otten 2019) as malfunctions of the plants have been described due to scaling. The geothermal plants M2 to M5 are kept under pressure to avoid degassing and mineral precipitation (Vetter 2012).

Chloride concentrations in deep fluid samples from the Malm in the MB range from 70 to 274 mg L^{-1} with a slight increasing trend with increasing depth. Fluoride and bromide concentrations range from 2.19 to 6.38 mg L^{-1} and 0.29–3.68 mg L^{-1} , respectively, with no correlation with depth. Sulfate concentrations range from 5.62–39.7 mg L^{-1} , with higher values in deeper fluid samples. There is a general trend of increasing temperatures with increasing well depth with minimum and maximum well depth corresponding to 2250 m and 4083 m, respectively, and the lowest and highest temperatures

corresponding to 65 °C and 135 °C, respectively (Table 5). DOC values range from 0.35–30.1 mg CL⁻¹ (Fig. 8). The three sites with depths between 2250 m and 3014 m report the lowest values, while the other sites of the MB show higher DOC values. The significantly higher DOC values in M4 and M4.1 possibly correlate with the occurrence of oil at this site as mentioned by Vetter (2012). The sites M4, M7 and M8 are in close vicinity to each other (all approximately within a 20 km radius). While M7 shows even higher DOC concentrations than M4, the site M8 has the lowest DOC in this group.

The variation in DOC concentration between M4, M7 and M8 might be due to the differing depths of the production wells being 3443 m, 3882 m, and 4083 m, respectively. Formate concentrations are generally low or below detection limit. Values are ranging from 0.03 to 0.72 mg CL⁻¹. The higher values are reported for the sites M4 and M7. Acetate concentrations range from 0.12–4.89 mg CL⁻¹. Again, the first three sites show very low to non-detectable acetate concentrations, whereas the other sites can be distinguished with significantly higher concentrations. Propionate ranges from 0.05–1.17 mg CL⁻¹ and occurs in M4, M4.1, M5, M7, and M8. Butyrate concentrations range from 0.07–0.35 mg CL⁻¹ in M4, M4.1, M5, and M8, while valerate (0.11 mg CL⁻¹) is only reported in the sites M4 and M4.1 (Table 5).

In addition to a general increase of DOC concentrations with depth, an increase of LMWOA (sum of formate, acetate, propionate, butyrate, and valerate concentrations) is also observed (Vetter 2012). This can also be seen when the additional data from Leins et al. (2022) are included to their findings (Table 5). In both cases the dominant organic acid is acetate, which is a common observation in formation waters associated with oils (Carothers and Kharaka 1978; Means and Hubbard 1987). As LMWOA concentration of M7 is nearly as high as in M4, this might be evaluated as an indication that the formation water of M7 is in contact with oil. Oil–water contact is suggested to increase the LMWOA concentration in the fluids due to the release of hydrophilic

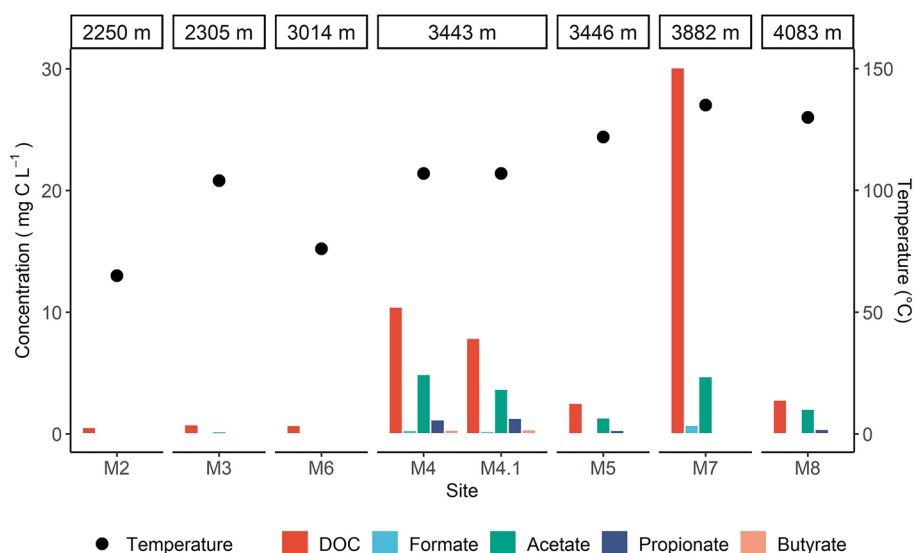


Fig. 8 Average DOC, formate, acetate, propionate, butyrate concentrations (mg CL⁻¹) and the temperature for each reported site of the Molasse Basin. The sites on the x-axis are arranged by the well depth (shallowest to deepest from left to right). Missing data represent either data below detection limit or not reported data

acids into the water (Reinsel et al. 1994). It was reported that the DOC composition changed with increasing depth (Vetter 2012). LMWNs were dominant in the shallowest fluid samples (M2) with relative abundance of 36% of the detected fractions and decreased with increasing depth to 8% in M5. Building blocks were dominant in M2 (32%) and M3 (41%), while LMWOAs dominated in the deeper and hotter fluids of the sites M4 and M5 with 64% and 67%, respectively. Biopolymers were present in M2, M3, and M4, however with a maximum relative abundance of only 2% in M2. Hydrophobic organic compounds were not detected.

It was stated by Vetter (2012) that the shift from the dominating fraction being the building blocks to LMWOAs with increasing depth and temperature can be explained by oxidation. Building blocks can be generated by alteration/degradation of humic substances and can be considered as an intermediate stage on the oxidation pathway to LMWOAs (Vetter 2012). In their study, they found humic substances in the DOC from the non-geothermal M1 site (240 m depth) in the Malm aquifer and made the assumption that with increasing depth of the Malm aquifer, the initially present humic substances are degraded into building blocks and further to LMWOAs as the final degradation product. In conclusion they explained that especially the deep Malm aquifer holds a large pool of potential substrates for microbial life due to dominating LMWOAs.

The risk of microbial induced corrosion or scaling could arise if certain conditions such as lower fluid temperatures are met. The Malm aquifer also provides sufficient amounts of electron acceptors such as sulfate and CO_2 as well as electron donors such as DOC, H_2S , and CH_4 for microbial metabolism (Vetter 2012). There is generally only minimal change in the concentrations of organic compounds when comparing samples from production and injection wells (Fig. 9). Noticeable, however is the change of DOC in M7, where the DOC decrease over a half from 30.1 mg CL^{-1} to 12.9 mg CL^{-1} . Several reasons can account for these differences. Sulfate reducing bacteria (SRB) were detected in the natural fluids in the production (106°C) and injection side (61°C) of M4, however with higher diversity on the injection side (Alawi et al. 2011). Thus, microorganisms may affect changes in organic compound composition. Naturally, the sulfate concentrations in the fluids from the production and injection side should reflect microbial activity with higher sulfate reduction rates on the latter side. However, high flow rates within the geothermal power plants of up to $100 \text{ m}^3 \text{ h}^{-1}$, provide continuous supply of organic substrates and electron acceptors such as sulfate as stated by Vetter (2012). Due to this, they explained that it is not possible to observe decreasing sulfate concentrations related to microbial sulfate reduction.

Organic compounds could also be influenced by abiotic processes within the geothermal power plant. Carbonate precipitations can occur in the power plants of the Molasse sites. Due to technical malfunctions the pressure will decrease leading to degassing of CO_2 and carbonate scaling. Those carbonate- or other scales can act as an adsorption surface for organic compounds (Thomas et al. 1993) and might affect DOC concentrations as well as their composition. In general, DOC composition shows a natural variability even when the geothermal plants are located in near distance. Here, the sporadic production of oil in only one geothermal system might explain the observed differences.

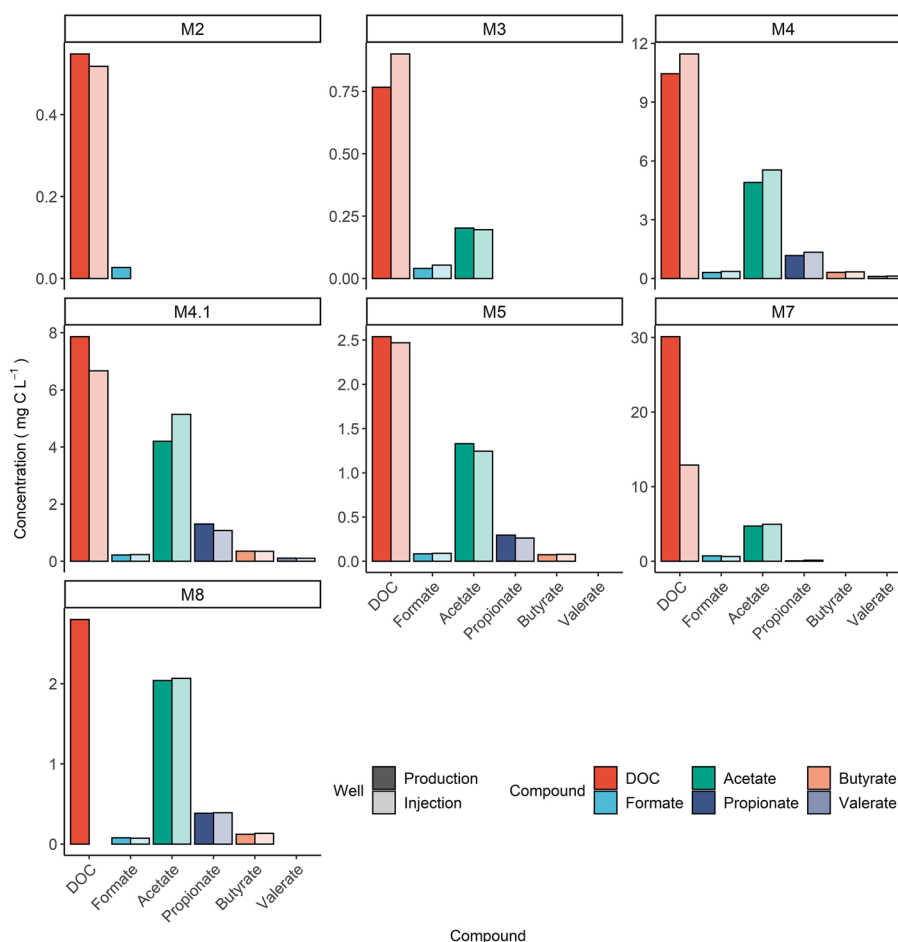


Fig. 9 Average DOC, formate, acetate, propionate, butyrate, and valerate concentrations (mg C L⁻¹) in samples from production (dark fill) and injection (clear fill) well of the Molasse Basin sites. Missing data represent either data below detection limit or not reported data

Geothermal fluids in the Upper Rhine Valley

The Upper Rhine Valley (URV) extends approximately 300 km from Frankfurt (Germany) to Basel (Switzerland). Its average width comprises 35 km and the valley forms part of an European rift system (Sanjuan et al. 2016). From the crystalline basement upwards, the URV is composed of granite (Cocherie et al. 2004) with overlying Mesozoic limestone and sandstone to Cenozoic evaporites and claystone (Sanjuan et al. 2016). Sequences with high permeability within the sedimentary section make up the major aquifers, of which the Triassic Buntsandstone is considered the most important (Aquilina et al. 1997). The general tectonic structure is characterized by nearly vertical faults that cross throughout the deep Triassic sediments to the Paleozoic crystalline basement (Baillieux et al. 2013; Pribnow and Schellschmidt 2000; Schellschmidt and Clauser 1996), allowing deep fluids circulation along these fractures (Sanjuan et al. 2016). A visual representation of a NW–SE cross-section of the Upper Rhine Valley is given in Fig. 10.

Fluids from deep geothermal wells of the URV are described as Na-Cl water type, with a pH value around 5.0, and total dissolved solids of 99 to 107 g L⁻¹ (Sanjuan et al. 2014, 2016). The fluids are described to be from multiple origin with a mixing

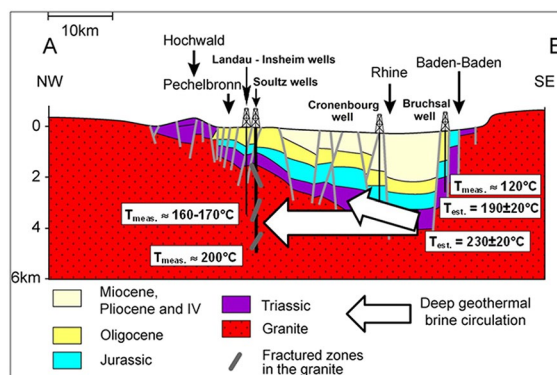


Fig. 10 Schematic NW-SE cross section of the Upper Rhine Valley (source Le Carlier (1994) and Sanjuan et al. (2010)) with several deep wells drilled to depths of 2540–5000 m. Estimated and measured temperatures ($T_{est.}$ and $T_{meas.}$) as well as deep geothermal brine circulation is represented in this cross section

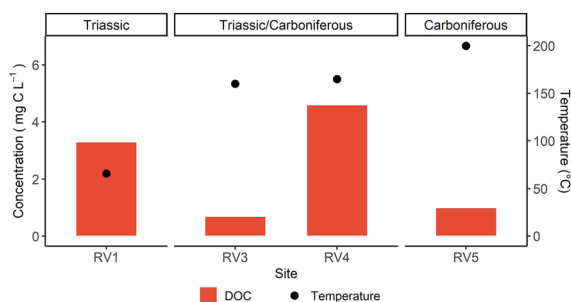


Fig. 11 Reported DOC concentrations and temperature for each reported site of the Upper Rhine Valley with samples from the production side

of primary marine brine and water of meteoric origin (Aquilina et al. 1997; Pauwels et al. 1993; Sanjuan et al. 2010, 2014; Vidal and Genter 2018).

DOC concentrations in geothermal fluids from the production side of the Upper Rhine Valley were reported for the sites Riehen (RV1), Landau (RV3), Insheim (RV4) (Sanjuan et al. 2016), and Soultz (RV5) (Sanjuan et al. 2014). One sample from the injection side was reported for Rittershofen (RV2) (Dezayes et al. 2013). The temperature increases with depth from 66°C (RV1 with 1547 m) to 200°C (RV5 with 5000 m). However, the temperature increase stagnates when comparing the well depths of RV3 and RV4 (Fig. 11). RV1 targets the Triassic Upper Muschelkalk, RV3 to RV4 the Triassic Buntsandstone and underlying fractured Carboniferous Granite, and RV5 the Carboniferous Granite of the URV. DOC concentrations are generally low (0.7 mg CL^{-1} in RV3 to 4.6 mg CL^{-1} in RV4) (Fig. 11).

The DOC concentrations reported for RV1, RV3, RV4, and RV5 originate from a single sample from each site. Since the data for the Upper Rhine Valley sites are very few, they might not represent the average DOC concentrations in the fluids of the sites. DOC concentrations show no correlation with either temperature or depth.

The use of scaling inhibitors was reported in RV2 and RV5 (Mouchot et al. 2018), and RV4 (pers. comm. of the plant operator). As previously mentioned, scaling inhibitors consisting of organic compounds will affect the DOC concentration of the fluid.

Here, also the point of inhibitor addition has to be taken into account when evaluating the effect of inhibitors on DOC composition and concentration. In RV4 the inhibitor is added before the heat exchanger, but the sampling point for the produced fluids is located prior to the injection point of the inhibitor. Therefore, the DOC of the production side samples in RV4 is not affected by the inhibitor. Unfortunately, the injection point of the scaling inhibitors is not described at RV2 and RV5. However, the samples for RV2 and RV5 were taken in January 2013 and June 2013, respectively. Inhibitor use at these sites started in November 2017 and October 2017, respectively (Mouchot et al. 2018). Therefore, DOC has not been influenced by any inhibitor at sites RV 2 and RV5. Fluid production in the URV is generally associated with scale formations (e.g., barite/celestine and minor formations of metal-rich deposits) (Mouchot et al. 2018; Scheiber et al. 2019). This might lead to application of inhibitors also in sites RV 3 and RV1. But to date, no information is available about the use of inhibitors at these sites.

Sample from injection side of RV2 showed a DOC concentration of 35.2 mg CL^{-1} . During the sampling, drill operations were still ongoing (tiefegeothermie.de 2021b) and environmental friendly chemicals were used to stimulate the reservoir. Therefore, it is likely that the sample from site RV2 is influenced by the drilling operation and the chemicals that were used for the reservoir stimulation. The sample at RV4 was taken approximately 1 month after an operational shutdown and maintenance time that lasted for several months (tiefegeothermie.de 2021a). Here, it is also likely that the reported DOC concentration of 4.6 mg CL^{-1} might not represent the natural DOC of the fluids.

Another explanation for the high DOC value in RV2 could be the proximity to the Pechelbronn oil-field. The best source rocks in this oil-field are of Toarcian age (Ledésert et al. 1996). Migration phenomena were reported to affect the Muschelkalk layers due to fault zones (Espitalié et al. 1988). RV3 targets the fractured Triassic Buntsandstone and Carboniferous fractured Granite. Hydraulic connections between the Muschelkalk and underlying Buntsandstone due to locally restricted fault systems and fractures could lead to water–oil contact. An artesian oil outflow was reported in a borehole in RV5 from a fractured zone in the Buntsandstone layers overlying the granite (Ledésert et al. 1996). They also found an organic-rich fractured zone in the granite at 2160 m depth, belonging to a fault system found between 2150–2180 m. However, RV5 is also located in the vicinity of the Pechelbronn oil-field as well as to the site RV2 and in comparison shows very low DOC concentrations. The influence of oil in the Muschelkalk or Buntsandstone from migration along fractures, and even the organic-rich zone in the granite might be of lesser importance for the geothermal well at RV5 since its depth reaches 5000 m into the granitic basement.

Another oil-field (Landau field) is located in the vicinity of RV3 and RV4, however both sites exhibit low DOC concentrations. Oil wells of RV3 target Eocene and Oligocene reservoirs in depths that range between 850–1500 m (Sanjuan et al. 2016), while geothermal fluids are produced from the granitic basement and Bunter layers at depths exceeding 3000 m. It was reported that the Landau oil field also produces oil from fractured Muschelkalk limestone and Keuper sandstone (Böcker et al. 2017; Schad 1962). Oil in the Muschelkalk might affect the DOC in the geothermal fluids of RV3 and RV4 if water–oil contact exists. The higher DOC concentration in RV4 (4.6 mg CL^{-1}) might

indicate that only RV4 is influenced by oil in the deeper formations from the Landau oil field. Even in proximity to each other with 5 km at the surface, both sites (RV3: 3044 m, RV4: 3600 m) have differing well depths. They could be connected to different fracture system of which only RV4 has a hydraulic connection to the oil producing sequences from the Muschelkalk of the Landau oil field. Sanjuan et al. (2016) concluded that the high concentrations of organic compounds within the granite basement were only possible if the basement was in hydraulic contact with the Mesozoic sediment.

GC–MS analyses of extracted organic matter by organic solvents from granitic rock samples from the organic-rich zone in the granite (2150–2180 m) of a deep drill hole in RV5 revealed various organic species (Ledésert et al. 1996). They obtained 48 mg of soluble lipids from a 418 g rock sample (0.12 mg/g). They were identified as 36.8% aliphatic acids, 18.5% aliphatic hydrocarbons, 41.3% alkylbenzenes, and 3.4% benzene dicarboxylic acids. The monocarboxylic acids in the C₉–C₃₂ range with highly dominant C₁₆ and C₁₈ and mainly even members were attributed to biogenic origin. However, the C₁₆H₃₀O₄ diester was considered as pollution from chemicals used for the drilling operation.

Two assumptions were made to explain the presence of organic matter in the granite (Ledésert et al. 1996): (a) the whole organic matter was transported downwards from the immature sediment formations overlying the granite due to fault-driven fluid circulation. The *n*-alkanes would result from thermal alteration of this organic matter in the granite due to the high geothermal gradient, while long chain aliphatic acids must have been transported more quickly since they would have been more susceptible to thermal degradation with a longer residence time in the granite. Alkylbenzenes were explained to also have been brought in through downward transportation since their distribution showed no evidence that they were derived from transformation of aliphatic monocarboxylic acids species present in the granite. If the alkylbenzenes were produced in situ they would have shown a distribution comparable to that of the aliphatic monocarboxylic acids but displaced by one carbon atom (Ji-Zhou et al. 1993; Ledésert et al. 1996). The second assumption (b) to explain the organic matter in the granite by Ledésert et al. (1996) was, that only a part of the organic compounds originated from the immature sediments (long *n*-alkanes, long chain aliphatic monocarboxylic acids), since the shorter *n*-alkanes showed great similarity in their distribution with detected *n*-alkanes from oil samples of the fractured sedimentary layers (Ledésert et al. 1996). More in-depth analyses of the DOC composition from the produced fluids in the URV might help to better understand the origin and fate of the organic compounds and with this, the fluid dynamics.

Bad Blumau, Austria

Data of DOC concentrations were compiled for the three individual sites Bad Blumau, Austria (S1), Klaipeda, Lithuania (B1), and a third anonymized site V1 which is also located in Austria (Vienna Basin). Bad Blumau is situated in south-east Austria and targets fluids from Paleozoic carbonate in the Styrian Basin in a depth of 2800 m and with temperatures of 107 °C. The fluids have a reported TDS of 20 g L⁻¹ and correspond to the Na-HCO₃ type (Westphal et al. 2019), with chloride concentrations of 3.3 g L⁻¹, sodium with 5.4 g L⁻¹, sulfate with 500 mg L⁻¹ and hydrogencarbonate with 8.2 g L⁻¹.

Their DOC data show significantly higher values in the production side with 14.5 mg CL^{-1} and 3 mg CL^{-1} in the injection side. It was reported that a biodegradable scaling inhibitor (Total organic carbon (TOC) = 190 g CL^{-1}) was added to prevent carbonate scaling. The inhibitor was injected at 500 m depths in the production well (Goldbrunner 2005) at a concentration of 10 mg L^{-1} , which resulted in a contribution to the DOC concentration of the fluid by approximately 1.6 mg CL^{-1} . The decrease in DOC from the production to the injection side was explained by microbial degradation.

Active microbial communities such as fermentative, sulfate reducing, and hydrogen oxidizing bacteria were reported already in the 107°C hot fluids (Westphal et al. 2019). An increase in the abundance of bacteria and sulfate reducers was observed with decreasing temperatures and explained by the heat extraction (down to 47°C) in the geothermal power plant. Furthermore, the additional organic carbon from the scaling inhibitor was reported to be most likely being degraded by those microorganisms. Except for a slight increase in H_2S concentrations which could lead to corrosion, no other compromising effects of the microbial activity within the power plant were detected (Vetter 2012).

Klaipeda, Lithuania

Klaipeda is situated at the coast of Lithuania. The Klaipeda geothermal power plant targets fluids from Lower Devonian Kemeris sandstones in the Baltic Sea Basin in depths of 1100 m, which is also the oldest geothermal used fluid in Europe to date (Brehme et al. 2019). The produced fluids reach temperatures of 38°C and were used for heat production. Total dissolved solids in the fluid are reported at 90 g L^{-1} and described as hyper-saline brine with a chloride content of around 60 g L^{-1} , with sodium accounting for two-thirds of the cation charge balance, while calcium and magnesium account for one-third (Brehme et al. 2019).

Here, DOC was reported to typically range from 1.6 to 2.4 mg CL^{-1} . Few samples, taken in spring 2016, showed lower DOC values. It was suggested that the scaling inhibitor acted as source of organic carbon and phosphate. The inhibitor was used to prevent gypsum scaling and was injected in the production side (Brehme et al. 2019). However, it is not clear if the inhibitor was also used during the 2-day sampling campaign in 2016. One sample taken from the injection side, had very high DOC of 139.7 mg CL^{-1} . However, this sample was taken from the fluid after flowing through a filter system. The sample taken from the injection side before the filter system only had a DOC of 0.66 mg CL^{-1} . DOC in fluids taken behind the filter system consisted of 74% LMWOA, 22% HOC and 4% LMWNs. It is assumed that microorganisms were present in the filter system and accounting to the DOC of the fluids passing through. Prior to this sampling campaign the Klaipeda site was not in use for several months and was only started up for the 2 days of sampling, which might explain the presence and activity of microorganisms in the filter system. In general, during normal operation of this site Brehme et al. (2019) observed microbial activity (sulfate reducing bacteria and archaea) with higher activities on the cooler injection borehole environment.

V1, Austria

V1 is situated near Vienna in Austria and targets relatively young fluids from Middle Miocene aquifer in the Vienna Basin in a depth of 900 m (Wessely 1983; Zekiri 2011). The produced fluids reach temperatures of 53 °C and are mainly used for balneological purpose and heat production. DOC is slightly higher in the samples from the injection side (0.35 mg C L⁻¹ to 1.11 mg C L⁻¹) than the production side (Leins et al. 2022).

Los Humeros, Mexico

The geothermal field Los Humeros is situated in the eastern part of the Trans-Mexican Volcanic Belt and considered a supercritical system (Reinsch et al. 2017). Temperatures are estimated to range from 300 to 400 °C. The litho-stratigraphic units of this field were characterized to consist of four main sequences. A sedimentary basement (limestone and metamorphic shale), the pre-caldera (lavas of mainly andesitic composition), rhyolitic ignimbrite deposits and some andesitic–dacitic–rhyolitic lavas, and post-caldera deposits of basaltic or basaltic–andesitic composition (Norini et al. 2015).

The geothermal fluids are considered to be mainly hosted in the andesite fracture of the pre-caldera (Peiffer et al. 2018). Fracture controlled secondary permeability in the reservoir was described to exist due to the complex volcanotectonic fault system in this region (Norini et al. 2019), allowing fluid circulation across sequences. Furthermore, noble gas analyses suggested that the produced fluids are composed of a mixture of at least four different components: local modern water recharge, deep fluid mining heat of an active magma source, fossil water from fluid circulation within the metacarbonate basement, and the last component most likely is represented by re-injected fluids (Pinti et al. 2017).

Ten condensates of vapor–water mixture (Table 6) from different production wells with depths ranging from 1770 to 2830 m were sampled (Sánchez-Avila et al. 2021). Condensates of water–vapor mixture were taken directly from the geothermal wellhead using a cooling coil of stainless steel. Organic matter was extracted from these samples with organic solvents for GC–MS analyses.

They identified 48 organic compounds from 6 homologous series, belonging to (in order of predominance) *n*-alkanes, aromatics, S-bearing and O-bearing hydrocarbons. Further investigation of the aromatic hydrocarbons revealed also the occurrence of compounds with two or more aromatic rings. The carbon chain length of the 24 identified *n*-alkanes ranged from C₁₀ to C₃₃ with high concentrations of *n*-alkanes ≤ _nC₂₄ in all samples. The calculated average chain length (ACL) ranging from 13.7 to 19.8, indicated an algae/bacterial input (Strauss et al. 2015), originating from organic matter buried in the reservoir rock (Sánchez-Avila et al. 2021). The presumable source of the organic matter, which is transformed into *n*-alkanes, are the fossiliferous limestone reservoir rocks between 1200–1210 m depth (Gutiérrez-Negrín et al. 2010; Norini et al. 2019). The terrigenous/aquatic ratio (TAR-HC) of the condensate samples revealed a high input of the *n*-alkanes from aquatic sources, suggesting that the origin was related to aquatic algae and detritus from the limestone reservoir rock (Sánchez-Avila et al. 2021). Only a sample from one well showed a TAR-HC ratio related to terrigenous derived *n*-alkanes, which was accounted by injection water.

Table 6 Overview of compiled data on organic matter in geothermal fluids from the Los Humeros (Mexico), Mutnovskii and Annenskii (Russia) geothermal fields

Well	Sample	Well depth (m)	Reservoir depth (m)	Discharge temperature (°C)	Reservoir temperature (°C)	Type of reservoir rock	Geological formation	No. of organic compounds	Range of n-alkanes	CPI
Los Humeros, Sánchez-Avila et al. (2021)										
			1150–2800		300–400 ^a	Pre-caldera andesites	Neogene Quaternary	48 (6 homologues)		
H-7	Condensate	2782		348					C10–C33	0.68
H-9	Condensate	2752		320					C10–C33	0.52
H-20	Condensate	2830		301					C10–C33	0.48
H-31	Condensate	1926		331					C10–C33	0.64
H-39	Condensate	2290		336					C11–C31	0.57
H-44	Condensate	1770		312					C10–C33	0.46
H-45	Condensate	2280		323					C10–C33	0.70
H-49	Condensate	2030		292					C11–C32	0.65
H-50	Condensate	2580		319					C10–C33	0.54
H-56	Condensate	1930		314					C10–C32	0.65
Mutnovskii, Kompanichenko et al. (2016)										
4-E/Dachnyi	Condensate	1600	1600–2000	175	270	Volcanic and volcano sedimentary	Oligocene Quaternary	48 (9 homologues)	C10–C26	-
no. 3/Severo	Condensate	1800		97	300–310			22 (5 homologues)	C10–C18 C23–C28	-
Annenskii, Poturay (2017)										
Well 21	Water	202	2000–3000	54	99 ^b	Volcanic and tuff sedimentary	Upper Cretaceous	72 (13 homologues)	C10–C14 C17–C32	0.95
Well 2	Water	44	2000–3000	54	99 ^b				C10–C14 C17–C35	0.9

^a Based on calculations of stabilized temperatures by the sphere method adjusted by PPEP (pressure profile versus depth) method (Gutiérrez-Negrín et al. 2010).^b Estimated by quartz thermometer (Kulakov 2014).

The high concentration of aromatics, low concentrations of *n*-alkanes, and the absence of cycloalkanes in 9 of the 10 condensates was interpreted by a strong involvement of aromatics forming pathways (Sánchez-Avila et al. 2021). They considered the hydrothermal alteration of buried organic matter as the possible origin for aromatic compounds, and was further supported due to the presence of phenalene, fluorene and fluoranthene, and a Carbon Preference Index (CPI) below 1. It represents the ratio of odd- to even-numbered *n*-alkanes and gives insight into the alteration of the organic matter. A CPI much greater than one suggests immaturity of the organic matter due to higher plant contribution, while a CPI approaching one indicates increasing maturity (Killops and Killops 2005).

Although the high temperatures of the Los Humeros geothermal field would not permit the existence of microorganisms, it was not discarded that microorganisms might exist in the lower temperature regions of the system. They could be involved in the production of organic matter that would be transported into the hotter regions of the system by fluid circulation (Sánchez-Avila et al. 2021).

Conclusively, Sánchez-Avila et al. (2021) described that their findings on organic compounds from the Los Humeros geothermal field condensates agreed with findings from condensates from the Kamchatka Peninsula hydrothermal fields in Kompanichenko et al. (2016). They differed in their proportions of the identified organic compounds, which was explained by Sánchez-Avila et al. (2021) due to the high temperature in the reservoir of the Los Humeros geothermal field and its water–rock interactions.

Geothermal sites in Russia

Data regarding the presence and relative concentrations of organic compounds in hot spring water and condensates from geothermal well samples from Kamchatka (Russia) hydrothermal fields were reported in Kompanichenko et al. (2016) and Poturay and Kompanichenko (2019). Here, two major hydrothermal systems are described, the Mutnovskii and the Uzon caldera, of which only the Mutnovskii area is being used to produce electricity. The Mutnovskii geothermal area is located in the southern part of the East Kamchatka volcanic belt and is composed of volcanic and volcanic sedimentary rocks of the Oligocene to present age (Poturay and Kompanichenko 2019). The area contains three distinct thermal fields: The Donnyi field within the crater of the Mutnovskii Volcano, the Severo-Mutnovskii, and Dachnyi both 3–4 km north of the crater. Each of those fields is described to host a great number of hot springs, mud pots, and vapor-gas vents. The geothermal power station operates within the Dachnyi and the nearby Verkhne-Mutnovskii thermal fields. Approximately 100 wells have been drilled with an average depth of 1.5 km, of which one-third is used as producing wells. The pressure and temperature were reported to reach up to 40 bar and 240 °C, respectively.

The chemical composition of the thermal waters sampled from the Dachnyi field was described as low mineral content, acidic, and of mixed cation composition; from Donnyi field as acidic water with higher chloride–sulfate and magnesium–calcium content; and from Severo-Mutnovskii as alkaline water with higher chloride, sulfate, and sodium content and also higher boric acid concentration (Kompanichenko et al. 2016).

In Kompanichenko et al. (2016), two condensate samples for DOM analyses were taken in the Mutnovskii area: one from a Dachnyi field well and one from a

Severo-Mutnovskii field well. After cooling of the samples, the DOM was extracted on site with the use of organic solvents. The extract was then analyzed via GC–MS in the laboratory. They yielded 95 organic compounds belonging to 16 homologous series, composed of mainly aromatic, oxygen-, chlorine-, and sulfur-containing hydrocarbons. In the condensate samples (4-E and no. 3) the *n*-alkanes ranged from C₁₀–C₂₈, most abundant (up to 85%) in the C₁₀–C₁₄ range. This group was described to be atypical for living organisms since bacteria synthesize odd homologues (C₇, C₉, C₁₁, C₁₃, and C₁₅) and not the even homologues in that range (Poturay and Kompanichenko 2019). The even-to-odd *n*-alkane ratio was close to one, which suggested that most of them were produced by thermocatalytic transformation of organic remnants (Kompanichenko et al. 2016). They supported this by the absence of both even carboxylic acids which are synthesized by bacteria, and steroids, ethers and terpenes which are regarded as biogenic markers. In comparison, samples from hot spring waters showed a more diverse composition. In addition to saturated and aromatic hydrocarbons those samples also contained biogenic carboxylic acids, their ethers, alcohols, terpenes, and steroids which was explained by the occurrence of thermophilic microorganisms (Kompanichenko et al. 2016).

Another geothermal site in Russia where DOM was characterized is the Annenskii geothermal field in the Khabarovsk territory (Poturay 2017). It is located in the northern part of the eastern Sikhote Alin volcanic belt consisting of Upper Cretaceous volcanic and tuff sedimentary rocks of the Bolbinskaya and Tatarkinskaya formations. It is overlain by a thin cover of Quaternary deposits consisting of loam, clay, and sand and is also characterized by numerous faults (Poturay 2017).

The geothermal field hosts about two dozen wells, of which two were producing ones during the study of Poturay (2017). The producing wells were Well 2 with 43.8 m depth and Well 21 with 201.6 m depth. Those geothermal fluids are only used for balneological purposes. The study describes the produced fluids as pressure fracture and veined-hosted waters originating from depth of up to 2–3 km with a reservoir and discharge temperature of approximately 99 °C and 54 °C, respectively. Furthermore, the fluids are described as weakly mineralized (mineralization < 0.3 g L⁻¹) and of alkaline silicic sulfate–carbonate sodic composition with elevated fluorine contents. A sample from each producing geothermal well was taken and analyzed via GC–MS after the DOM was extracted from those samples (Poturay 2017).

They yielded 72 organic compounds of 13 homologous series. Most typical compounds found in those samples were *n*-alkanes and esters, making up 20–50% of all organic compounds. Other identified compounds were alcohols, aldehydes, ketones, carboxylic acids, terpenes, steroids, and nitrogen bearing compounds. The identified *n*-alkanes ranged from C₁₁ to C₂₈. The resulting CPI calculated from the *n*-alkane abundance equaled around 0.9 and suggested a certain contribution of thermogenic organic compounds to the overall organic matter (Poturay 2017). However, the organic matter was described to be mainly of biogenic origin due to the overall identified organic compounds and, e.g., the suggested occurrence of thermophilic bacteria, and the Annenskii geothermal field being a zone for meteoric water recirculation. Based on the composition and distribution of *n*-alkanes they also calculated the percentage of *n*-alkanes synthesized from phytoplankton (*n*-C₁₇ and *n*-C₁₉) and from

bacteria (*n*-C₂₀ to *n*-C₂₄). This showed a contribution to the *n*-alkane composition of 1.9% and 0.6% from phytoplankton and 18.4% and 11.5% from bacteria in Well 21 and Well 2, respectively.

Comparison and integration of the data

Distribution of DOM in geothermal fluids

The available DOC concentrations across all of the here reported geothermal sites are presented in Fig. 12. It shows a similar trend of DOC concentrations with regard to the subsurface temperature as was described for aliphatic acid anions in oil-field waters (Carothers and Kharaka 1978; Kharaka et al. 1985b, 2000) (Fig. 3). In the temperature range of 30–80 °C, DOC and the sum of LMWOA concentrations do not exceed 10 mg CL⁻¹ and 0.6 mg CL⁻¹, respectively. Between 80 and 200 °C concentrations can be higher, however decreasing as temperatures reach up to 200 °C. Carothers and Kharaka (1978) attributed their generally lower LMWOA concentrations for temperatures below 80 °C to microbial degradation. This might be also a valid explanation for the data in this review for both DOC and LMWOA. As the temperatures increases, microbial species have to be more specialized to be able to survive in such environments (extreme thermophiles: 75–95 °C; hyperthermophiles: > 90 °C) (Sand 2003). The highest known temperature limit for microbial life lies at 122 °C (*Methanopyrus kandleri 116*) (Takai et al. 2008). Thus, microbial degradation of DOM becomes a less important factor with

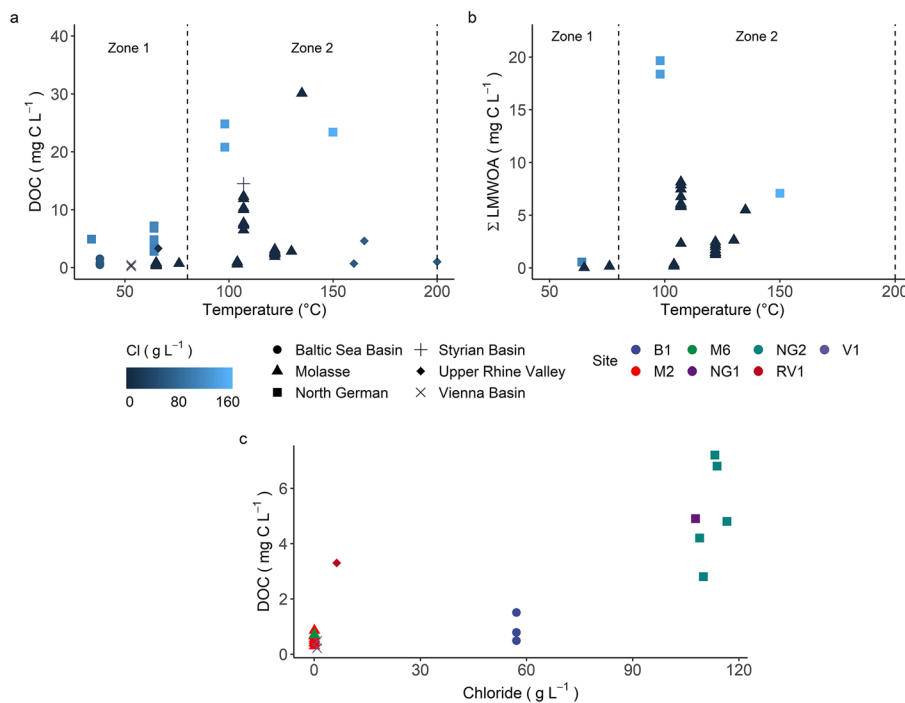


Fig. 12 **a** DOC, and **b** sum of organic acid anions vs. temperature, color-coded by chloride content (g L⁻¹). Temperature zones are marked according to Kharaka et al. (2000). **c** DOC vs. chloride content for the samples within the temperature range of 30–80 °C. For the Klaipeda geothermal site (B1, Baltic Sea Basin) no chloride concentrations were given for the respective DOC concentrations. Thus, the average chloride concentration from well data reported in Brehme et al. (2019) was used instead

increasing temperatures of up to 130 °C, where spontaneous decomposition of nucleic acids and proteins starts (Sand 2003). However, not only the temperature can be a limiting factor for microbial life, but also the pressure, pH, radioactivity, and salinity (Bregnard et al. 2022). Interestingly, the DOC concentrations compiled here within this lower temperature range (30–80 °C) seem to show a positive trend with the chloride content of the fluids (Fig. 12). This might suggest that with a higher salinity of the brine in the lower temperature range, the conditions for microbial life and microbial degradation of DOM are more limited. While microbial degradation could be the limiting factor for DOC concentration in the lower geothermal temperature ranges, the generally decreasing DOC within the range of 80–200 °C might be attributed to thermal degradation of the DOM as it was also pointed out in Carothers and Kharaka (1978).

Data from two high-enthalpy sites are presented from the Los Humeros, Mexico and Mutnovskii, Russia geothermal fields. The qualitative DOM analyses showed that in samples from both sites, aromatic hydrocarbons and *n*-alkanes were the dominant compounds found in the condensates. In the Los Humeros samples they also detected aromatic hydrocarbons with more than two rings (Sánchez-Avila et al. 2021). Generally, the findings from Los Humeros and Mutnovskii were described to be in good agreement with regard to the organic species that were identified, however in different proportions (Sánchez-Avila et al. 2021). In both sites the formation of the identified organic compounds was explained by thermogenic alteration of buried organic matter due to a CPI < 1 in the Los Humeros samples and the absence of steroids, ethers, terpenes, and even carboxylic acids in the Mutnovskii samples, which are regarded as biogenic markers (Kompanichenko et al. 2016). Compared to these two high-enthalpy sites, the Annenskii geothermal field with the two samples from 54 °C to 99 °C hot produced waters, showed that *n*-alkanes and esters were the dominating compounds (Poturay 2017). Here, the DOM was described to be mainly biogenic. They found that 11–18% of the *n*-alkane composition was formed by bacteria, which further solidifies that microorganisms might be present in geothermal fluids of lower temperature sites. All three sites had *n*-alkanes dominating compound, however aromatic hydrocarbons formation seems more favorable in the high-enthalpy sites. However, the interpretation of this data with regard to DOC has to be viewed with care for these three sites. In the description of the sampling process and preparation, there was no mention of filtering of the fluid samples. In this case, the organic matter detected in their analyses might be influenced by particulate organic carbon (POC). Samples from Sánchez-Avila et al. (2021), Kompanichenko et al. (2016), and Poturay (2017) might not only represent DOC and this has to be considered when comparing their findings with other data.

Origin of DOM in geothermal fluids

Several factors such as the use of chemical scaling inhibitors, operation time since start up of the power plant, operational stops due to maintenance of the surface installations, or the proximity and connectivity to oil-bearing, or organic-rich strata is important to consider when interpreting the origin of the DOM in geothermal used fluids. Contamination due to drilling operations and drilling mud was previously mentioned for RV2 and discussed for M5 in Vetter (2012). They showed high initial DOC concentrations in M5 fluids (4–10 mg CL⁻¹) within the first 16 months of plant operation. The following

15 months of monitoring, the DOC was stable at around 2 mg CL^{-1} . Contamination of the produced fluids due to drilling mud is likely given only during the early phase of a geothermal power plant. The amount of drilling mud left in the borehole and flow rates of the power plant would affect this period.

The DOC concentration and composition can be influenced by the addition of scaling inhibitors by adding artificial DOM on top of the natural DOM to the system as was reported in Bad Blumau (S1) (Westphal et al. 2019) and Klaipeda (B1) (Brehme et al. 2019). Oftentimes, the exact chemical composition of scaling inhibitors fall under the protection of commercial and industrial secrecy. In general, they are water-soluble polymers that can be injected into the geothermal fluid at any desired ratio (Zotzmann et al. 2018). In B1 the inhibitor was a diethylene triamine pentamethylene phosphonic acid (DTPMP or $\text{C}_9\text{H}_{26}\text{N}_3\text{P}_5\text{O}_{15}$) solved in water (Brehme et al. 2019). Ideally, inhibitors should remain stable until the decrease of the inhibitory effect would no more lead to scaling or reduction of injectivity in the geothermal power plant. A delayed degradation is desired to avoid their persistence or accumulation in the reservoir (Zotzmann et al. 2018). However, inhibitors might be subject to thermal or microbial degradation due to high temperatures of the geothermal fluids (Zotzmann et al. 2018) or microbial activity (Brehme et al. 2019; Westphal et al. 2019). If one or more inhibitors are in use, their point of injection in the system can vary from site to site and has to be taken into account for the evaluation of the fluid samples. In S1, for example (Fig. 4), the inhibitor is injected in approximately 500 m depth into the production well, while in RV4 the injection occurs right before the heat exchanger. All sampling points at S1 are located at the surface and thus all of the fluid samples are influenced by the inhibitor. At RV4 the sampling point for the production side is located prior to the inhibitor injection, meaning that those fluids samples are unaffected. However, samples from the injection side are affected from the inhibitor. If data would have been available from injection side fluids, the inhibitor injection might have been observable, giving a good estimate on the influence of the inhibitor on the natural DOM.

Hydraulic connectivity through fracture and fault systems within a sedimentary basin to organic-rich deposits might lead to significantly differing DOM composition and concentration in spite of geothermal sites targeting similar formations (Vetter 2012). Comparing the fluid samples from the NGB and MB, where data on short chain organic acid anion concentrations were available, propionate, butyrate, and valerate were generally only present in the MB sites M4, M4.1, M5, and M8 (Fig. 13). They show a decrease in abundance from acetate to valerate (low to higher carbon number) with acetate as dominant organic acid anion, which is in good agreement with the data from oil-field waters (Carothers and Kharaka 1978; Hatton and Hanor 1984; Kharaka et al. 1985b, 2000). In deep sediments, different pathways are known to describe their origin. Thermal degradation of kerogen (Barth et al. 1988; Kawamura et al. 1986; Lundegard and Kharaka 1990), thermal maturation of petroleum source rocks, oil, and immature sedimentary rocks (Borgund and Barth 1994; Kharaka et al. 1993; Seewald 2001), and hydrolysis of macromolecular organic matter such as kerogen (Glombitza et al. 2009). However, it was suggested that LMWOAs either derive from thermal cracking reactions by alteration of large molecules into smaller groups by temperature (Barth et al. 1988), from oxidation of *n*-alkanes (Seewald 2001), or

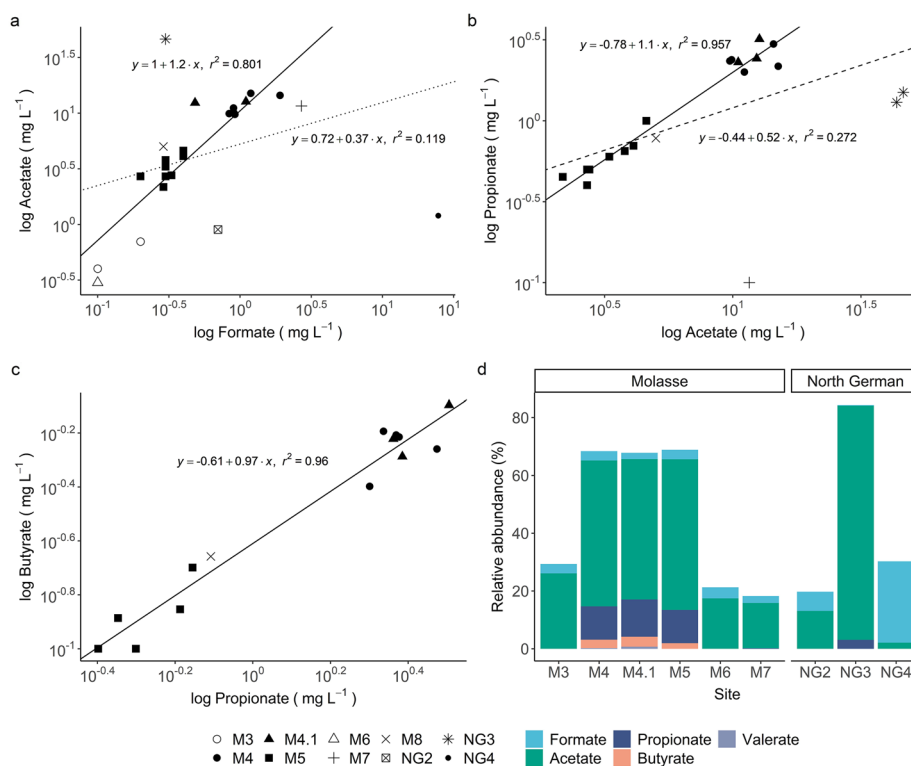


Fig. 13 Logarithmic plots of a) formate and acetate (dotted and solid line represent a regression with all data and only Molasse Basin data, respectively). b) Acetate and propionate (dashed and solid line represents a regression with all data and without NG3 and M7, respectively). c) Propionate and butyrate concentrations from the Molasse and North German Basin. d) Mean relative abundance of organic acid anions with regard to the DOC concentrations in the fluid samples

from hydrolysis of cross-linked esters within the macromolecular network of kerogen (Siskin and Katritzky 1991). In this case the presence of acetate, propionate, butyrate, and valerate (in decreasing abundance) could be an indicator that the DOM in fluids might originate from oil–water contact. M4 and M4.1, which show the highest concentrations of organic acid anions in the MB, were described to incidentally produce oil in addition to the hot water (Vetter 2012), further reinforcing the assumption of oil affected DOM in those fluids.

In the NGB samples, high concentrations of acetate (18.29 mg CL^{-1}) and formate (6.6 mg CL^{-1}) were only reported for NG3 and NG4, respectively. Only NG3, showed also slight traces of propionate in the NGB, however with a LMWOA abundance above 80% mostly dominated by acetate, compared to the MB sites (Fig. 13). A linear trend in log–log plotted acetic/propanoic acid and propanoic/butyric acid concentrations from various oil-field brines was also shown in Seewald (2001). With additional experimental data, they concluded that short chain carboxylic acids in sedimentary oil-field waters most likely form through a series of reaction where aqueous *n*-alkanes are oxidized to *n*-alkenes, alcohols, ketones, and carboxylic acids as intermediates. In this review, also the formate and acetate concentrations were log–log plotted (Fig. 13). It shows that the MB sites follow a linear trend, while NG2 and NG3 are more scattered, and NG4 lies far from the other data points with its high formate over acetate

dominance. Interestingly, the acetate/propionate plot shows NG3 and M7 as strongly scattered compared to the rest of the data points. In combination, both the formate/acetate and acetate/propionate plots might suggest that for NG2, NG3, NG4, and M7 DOM was introduced artificially into the system such as by the injection of a chemical inhibitor. These formate, acetate, and propionate concentrations might have also been the product of organic acid producing microorganisms. However, microbial activity in the production fluids of M7 and NG4 with temperatures of 135 °C and 150 °C, respectively, seems unlikely compared to NG3 with 98 °C. Another explanation could be the abiotic synthesis of carboxylic acids due to water–rock reactions. The absence of propionate, butyrate, and valerate in the lower temperature MB and generally all NGB fluids indicates that oil affected water as explanation for the DOM composition most likely can be excluded for these sites. The relative abundance of organic acid anions in Fig. 13 could serve as an additional indicator for this assumption. Only in M4, M4.1, and M5, organic acid anions have a similar distribution and together, form over 60% of the DOC in the fluids. Finally, the log–log plots and the abundance of organic acid anions suggests that only for M4, M4.1, M5, and M8, water–oil contact is a valid explanation as part of the origin of the DOM. Interestingly, the site M3 shows similar DOC and organic acid anion concentrations below 1 mg CL⁻¹ as the lower temperature sites in the MB and NGB, however with a temperature of 106 °C which fits into the MB sites who presumably exhibit water–oil contact. Compared to the rest of the MB sites, M3 is located in Austria and not clustered as the other sites. No water–oil contact or connection to organic-rich deposits due to the differing locality, in addition to thermal degradation and low natural DOM of the fluids could explain the low DOM content in M3.

Implications of DOM in geothermal fluids

A problem that available DOM in the fluids poses to the operation of a geothermal power plant is, that it serves as nutrient for microorganisms. Even geothermal sites with high temperatures might be affected, due to the ability of microorganisms to form spores that are more resistant to unfavorable conditions (Filippidou et al. 2019). While in this low-metabolic state, upon meeting more favorable conditions they can return to their full metabolic activity. A change from unfavorable to favorable conditions in a geothermal power plant is the heat extraction from the fluids. In S1 the decrease of DOC concentrations from the production to the injection side was attributed by microbial degradation, and in both S1 and M4 a higher abundance of microorganisms such as sulfate reducing bacteria were detected due to the change in fluid temperature (Vetter 2012; Westphal et al. 2019). An uncontrolled growth of the microbial community might lead to corrosion of the casing and formation of scales due to their metabolic byproducts, changing the fluid chemistry (Inagaki et al. 2003; Westphal et al. 2019). Biofilms can affect the flow rates and injectivity, due to clogging of pores and filters (Brehme et al. 2020; Ábel et al. 2021) and even heat exchangers might lose their capacity as biofilms within the heat exchanger create an insulating effect at the surfaces where they are formed (Sand 2003). Comparing and monitoring the inorganic composition, DOM content as well as microbial abundance and diversity between the production and injection side can be crucial to detect and mitigate the operational problems that would result from microorganisms

present in the fluids of a geothermal power plant. In S1 for example, this approach led to the observation that H₂S concentrations increased slightly due to microbial activity in the geothermal fluids (Westphal et al. 2019), which in greater concentrations can lead to corrosion effects on the casing and pipes.

Conclusion

A total of 143 fluid samples from 22 geothermal sites were presented and discussed leading to the following conclusions in this review. Aromatic compounds seem to be the dominant organic species in high-temperature geothermal systems while *n*-alkanes are dominant in low-temperature systems. The DOC and LMWOA concentration in low- to medium-temperature sedimentary basin reservoirs show a similar distribution with temperature as aliphatic acid anions in oil-field brines. Lower DOC and LMWOA concentrations are found below 80 °C with higher concentrations above 80 °C and decreasing towards 200 °C. Microbial degradation of DOM in the lower temperature ranges (30–80°C) appears to be the main factor for lower DOC concentrations, while the thermal degradation of DOM accounts for the decreasing DOC concentrations in the temperature range of 80–200°C. Higher salinity of the fluids might limit microbial activity, leading to higher possible DOM content in more saline brines. Hydraulic connections to organic-rich sediments or oil-bearing strata within the reservoir can be detected by investigating the DOM content and composition of the geothermal fluids. Especially, the occurrence of organic acid anions such as acetate, propionate, butyrate, and valerate, and their abundance might be a good indicator if geothermal fluids had been in contact with oil. The injection of chemical inhibitors contributes to the DOM content of the fluids, which might favor the formation of microbial communities in geothermal power plants with lower fluid temperatures. Monitoring the DOM content and formation of microbial communities within the power plants can help to avoid or mitigate operational problems caused by biofilms and biofouling. Collecting more data from various geothermal sites targeting different geological systems might help to get a better insight on which geothermal settings could be related to the occurrence of operational difficulties. Finally, this review shows that incorporating DOM analyses for geothermal fluids can be an important additional tool to better understand the fluid chemistry and reservoir conditions, and to optimize geothermal operation.

Abbreviations

DOM	Dissolved organic matter
TOC	Total dissolved carbon
DOC	Dissolved organic carbon
LMWOA	Low molecular weight organic acids
LC-OCD	Liquid chromatography organic carbon detection
bio	Biopolymers
Hs	Humic substances
BB	Building blocks
LMWN	Low molecular weight neutrals
HOC	Hydrophobic organic carbon
IC	Ion chromatography
GC-MS	Gas chromatography–mass spectrometry
NGB	North German Basin
CEB	Central European Basin
DAC	Deep aquifer complex
LPC	Low permeability complex
TDS	Total dissolved solids

MB	Molasse Basin
SRB	Sulfate reducing bacteria
URV	Upper Rhine Valley
ACL	Average carbon chain length
TAR-HC	Terrigenous over aquatic ratio of hydrocarbons
CPI	Carbon Preference Index

Acknowledgements

We wish to thank Alexandra Vetter for providing sample data from the Molasse and North German Basin, Maren Brehme for providing additional information and insights about the Klaipeda geothermal site, and Kristin Günther (GFZ Potsdam) for the laboratory analyses of the samples.

Author contributions

AL and DB made major contributions to the acquisition and analysis of the data. AL, DB, AVH, PJ, and SR made major contributions to the interpretation of the data. All authors read and approved the final manuscript.

Funding

Open Access funding enabled and organized by Projekt DEAL. This work has been funded by the European Union's Horizon 2020 research and innovation program within the framework of the REFLECT project under the grant agreement No. 850626.

Data availability

The datasets generated and/or analyzed during the current study are available in the GFZ data services repository, <https://doi.org/10.5880/GFZ.4.8.2022.001>

Declarations

Competing interests

The authors declare that they have no competing interests.

Received: 4 February 2022 Accepted: 26 May 2022

Published online: 25 June 2022

References

- Ábel M, Judit M-S, Maren B. Injection related issues of a doublet system in a sandstone aquifer—a generalized concept to understand and avoid problem sources in geothermal systems. *Geothermics*. 2021;97:102234. <https://doi.org/10.1016/j.geothermics.2021.102234>.
- Alawi M, Lerm S, Vetter A, Wolfgramm M, Seibt A, Würdemann H. Diversity of sulfate-reducing bacteria in a plant using deep geothermal energy. *Grundwasser*. 2011;16(2):105–12. <https://doi.org/10.1007/s00767-011-0164-y>.
- Andrews J, Youngman M, Goldbrunner J, Darling W. The geochemistry of formation waters in the Molasse Basin of Upper Austria. *Environ Geol Water Sci*. 1987;10(1):43–57. <https://doi.org/10.1007/BF02588004>.
- Aquilina L, Pauwels H, Genter A, Fouillac C. Water-rock interaction processes in the Triassic sandstone and the granitic basement of the Rhine Graben: Geochemical investigation of a geothermal reservoir. *Geochimica et Cosmochimica Acta*. 1997;61(20):4281–95. [https://doi.org/10.1016/S0016-7037\(97\)00243-3](https://doi.org/10.1016/S0016-7037(97)00243-3).
- Bachmann GH, Müller M, Weggen K. Evolution of the Molasse Basin (Germany, Switzerland). *Tectonophysics*. 1987;137(1):77–92. [https://doi.org/10.1016/0040-1951\(87\)90315-5](https://doi.org/10.1016/0040-1951(87)90315-5) (**Compressional Intra-Plate Deformations in the Alpine Foreland**).
- Baillieux P, Schill E, Edel J-B, Mauri G. Localization of temperature anomalies in the Upper Rhine Graben: insights from geophysics and neotectonic activity. *Int Geol Rev*. 2013;55(14):1744–62. <https://doi.org/10.1080/00206814.2013.794914>.
- Barth T, Borgund AE, Hopland AU, Graue A. Volatile organic acids produced during kerogen maturation— amounts, composition and role in migration of oil. In: Mattavelli L, Novelli L, editors. *Organic geochemistry in petroleum exploration*. Amsterdam: Pergamon; 1988. p. 461–5. <https://doi.org/10.1016/B978-0-08-037236-5.50053-1>.
- Beer H, Manhenke V. Erdwärme-und Thermalsolenutzung in Ostbrandenburg. *Zeitschrift für geologische Wissenschaften*. 2001;29(1/2):211–22.
- Böcker J, Littke R, Forster A. An overview on source rocks and the petroleum system of the central Upper Rhine Graben. *Int J Earth Sci*. 2017;106(2):707–42. <https://doi.org/10.1007/s00531-016-1330-3>.
- Bodvarsson G. Physical characteristics of natural heat resources in Iceland. *Jökull*. 1961;11:29–38.
- Boles JR. Active ankerite cementation in the subsurface Eocene of southwest Texas. *Contributions Mineralogy Petrology*. 1978;68(1):13–22. <https://doi.org/10.1007/BF00375443>.
- Borgund AE, Barth T. Generation of short-chain organic acids from crude oil by hydrous pyrolysis. *Org Geochem*. 1994;21(8):943–52. [https://doi.org/10.1016/0146-6380\(94\)90053-1](https://doi.org/10.1016/0146-6380(94)90053-1).
- Bregnard D, Leins A, Cailleau G, Vieth-Hillebrand A, Eichinger F, Ianotta J, et al. Microbial life in deep geothermal fluids— a review on occurrence, diversity and challenges for its analysis. *Geotherm Energy*. 2022.
- Brehme M, Nowak K, Banks D, Petrauskas S, Valickas R, Bauer K, Burnside N, Boyce A. A review of the hydrochemistry of a deep sedimentary aquifer and its consequences for geothermal operation: Klaipeda, Lithuania. *Geofluids*. 2019. <https://doi.org/10.1155/2019/4363592>.

- Brehme M, Nowak K, Abel M, Siklosi I, Willems C, Huenges E. Injection Triggered Occlusion of Flow Pathways in a Sedimentary Aquifer in Hungary. World Geothermal Congress 2020, WGC 2020 ; Conference date: 21-05-2020 Through 26-05-2020; 2020. <https://www.wgc2020.com/>
- Butturini A, Amalfitano S, Herzsprung P, Lechtenfeld OJ, Venturi S, Olaka LA, Pacini N, Harper DM, Tassi F, Fazi S. Dissolved organic matter in continental hydro-geothermal systems: insights from two hot springs of the East African Rift Valley. *Water*. 2020. <https://doi.org/10.3390/w12123512>.
- Carothers WW, Kharaka YK. Aliphatic acid anions in oil-field waters—implications for origin of natural gas. *AAPG Bull.* 1978;62(12):2441–53. <https://doi.org/10.1306/C1EA5521-16C9-11D7-8645000102C1865D>.
- Carothers WW, Kharaka YK. Stable carbon isotopes of HCO₃ in oil-field waters—implications for the origin of CO₂. *Geochimica et Cosmochimica Acta*. 1980;44(2):323–32. [https://doi.org/10.1016/0016-7037\(80\)90140-4](https://doi.org/10.1016/0016-7037(80)90140-4).
- Cocherie A, Guerrot C, Fanning C, Genter A. U-Pb dating of two granite types from Soultz (Rhine Graben, France). *Comptes Rendus Geoscience*. 2004;336(9):775–87. <https://doi.org/10.1016/j.crte.2004.01.009>.
- Demir MM, Baba A, Atilla V, Inanli M. Types of the scaling in hyper saline geothermal system in northwest turkey. *Geothermics*. 2014;50:1–9. <https://doi.org/10.1016/j.geothermics.2013.08.003>.
- Dezayes C, Sanjuan B, Gal F, Lerouge C, Brach M. Forage d'exploration géothermique GRT-1. Suivi géochimique des fluides et caractérisation des zones fracturées. Rapport final BRGM/RP-62546-FR; 2013.
- Di Gioia M, Leggio A, Pera AL, Liguori A, Perri F. Occurrence of organic compounds in the thermal sulfurous waters of Calabria, Italy. *Chromatographia*. 2006;63(11):585–90.
- Espitalié J, Marquis F, Barsonyi I, Fritz B. Diagraphie géochimique du forage géothermique de Soultz-sous-Forêts (GPK1) en Alsace. IFP Doc, 6; 1988.
- Feldbusch E. Geochemische Charakterisierung eines Formationsfluids im Unteren Perm. Doctoral thesis, Universität Potsdam; 2015. <https://publishup.uni-potsdam.de/frontdoor/index/index/docId/8740>
- Filip Z, Smed-Hildmann R. Does fossil plant material release humic substances into groundwater? *Sci Total Environ*. 1992;117–118:313–24. [https://doi.org/10.1016/0048-9697\(92\)90098-D](https://doi.org/10.1016/0048-9697(92)90098-D) (**Advances in Humic Substances Research**).
- Filippidou S, Junier T, Wunderlin T, Kooli WM, Palmieri I, Al-Dourobi A, Molina V, Lienhard R, Spangenberg JE, Johnson SL, Chain PSG, Dorador C, Junier P. Adaptive strategies in a poly-extreme environment: differentiation of vegetative cells in *Serratia ureilytica* and resistance to extreme conditions. *Front Microbiol*. 2019;10:102. <https://doi.org/10.3389/fmicb.2019.00102>.
- Fisher JB, Boles JR. Water-rock interaction in Tertiary sandstones, San Joaquin basin, California, U.S.A.: diagenetic controls on water composition. *Chem Geol*. 1990;82:83–101. [https://doi.org/10.1016/0009-2541\(90\)90076-J](https://doi.org/10.1016/0009-2541(90)90076-J).
- Franz M, Barth G, Zimmermann J, Budach I, Nowak K, Wolfram M. Geothermal resources of the North German Basin: exploration strategy, development examples and remaining opportunities in Mesozoic hydrothermal reservoirs. *Geol Soc London Special Publ*. 2018;469(1):193–222. <https://doi.org/10.1144/SP469.11>.
- Gast R, Pasternak M, Piske J, Rasch H-J. Das Rotliegend im nordostdeutschen Raum: Regionale Übersicht, Stratigraphie, Fazies und Diagenese. In: *Geologisches Jahrbuch Reihe A. Bundesanstalt Für Geowissenschaften und Rohstoffe, Hannover*; 1998. p. 59–80.
- Glombitza C, Mangelsdorf K, Horsfield B. A novel procedure to detect low molecular weight compounds released by alkaline ester cleavage from low maturity coals to assess its feedstock potential for deep microbial life. *Org Geochem*. 2009;40(2):175–83. <https://doi.org/10.1016/j.orggeochem.2008.11.003>.
- Goldbrunner J. Vergleich von Isotopenuntersuchungen an Tiefenwässern des Steirischen Beckens und des Oberösterreichischen Molassebeckens. *Mitteilungen der Österreichischen Geologischen Gesellschaft*. 1997;88:31–9.
- Goldbrunner JE. Hydrogeology of deep groundwaters in Austria. *Mitteilungen der Österreichischen Geologischen Gesellschaft*. 2000;92(1999):281–94.
- Goldbrunner J. Bad Blumau (Styria, Austria) The success story of combined use of geothermal energy. *Geo-Heat Centre (GHC) Q Bull*. 2005;26(2):27–30.
- González-Barreiro C, Cancho-Grande B, Araujo-Nespereira P, Cid-Fernández JA, Simal-Gándara J. Occurrence of soluble organic compounds in thermal waters by ion trap mass detection. *Chemosphere*. 2009;75(1):34–47. <https://doi.org/10.1016/j.chemosphere.2008.11.067>.
- Göthel M. Nutzung und Potenziale des tiefen Untergrundes in Brandenburg, Teil 2: Erdwärme-Erschließung durch Systeme der Tiefen Geothermie, Wärmespeicherung und Thermalsolegewinnung. *Brandenburg. geowiss. Beiträge*; 2014. p. 129–138.
- Gross D, Sachsenhofer R, Rech A, Sageder S, Geissler M, Schnitzer S, Troiss W. The Trattnach oil field in the north alpine foreland basin (Austria). *Austrian J Earth Sci*. 2015;108(2):151–71. <https://doi.org/10.17738/ajes.2015.0018>.
- Grunert P, Auer G, Harzhauser M, Piller WE. Stratigraphic constraints for the upper Oligocene to lower Miocene Puchkirchen Group (North Alpine Foreland Basin, Central Paratethys). *Newslett Stratigr*. 2015;48(1):111–33. <https://doi.org/10.1127/nos/2014/0056>.
- Gutiérrez-Negrín LC, Izquierdo-Montalvo G, Aragón-Aguilar A. Review and update of the main features of the Los Hornos geothermal field, Mexico. *Proceedings World Geothermal Congress, Bali, Indonesia, 25-29 April, 2010*; 2010.
- Hanor JS. Origin of saline fluids in sedimentary basins. *Geol Soci London Special Publ*. 1994;78(1):151–74. <https://doi.org/10.1144/GSL.SP.1994.078.01.13>.
- Hatton R, Hanor J. Dissolved volatile fatty acids in subsurface, hydropressure brines: a review of published literature on occurrence, genesis and thermodynamic properties. Technical Report for Geopressured-Geothermal Activities in Louisiana: Final Geological Report for the Period 1 November 1981 to 31 October 1982. DOE Report No. DOE/NV/10174-3; 1984.
- Henninges J, Brandt W, Erbas K, Moeck I, Saadat A, Reinsch T, Zimmermann G, et al. Downhole monitoring during hydraulic experiments at the in-situ geothermal lab Groß Schönebeck. *Proceedings of the thirty-seventh workshop on geothermal reservoir engineering. Stanford University, Stanford, California, January 30 - February 1, 2012, SGP-TR-194*; 2012.

- Huber B. Das Thermalwasservorkommen im niederbayrisch-österreichischen Molassebecken [The hydrothermal water in the Bavarian-Austrian Molasse Basin]. Report, Bayerisches Landesamt für Wasserwirtschaft, Munich, Germany; 1999.
- Huber SA, Frimmel FH. Size-exclusion chromatography with organic carbon detection (LC-OCD): a fast and reliable method for the characterization of hydrophilic organic matter in natural waters. *Vom Wasser*. 1996;86:277–90.
- Huber SA, Balz A, Abert M, Pronk W. Characterisation of aquatic humic and non-humic matter with size-exclusion chromatography - organic carbon detection - organic nitrogen detection (LC-OCD-OND). *Water Res*. 2011;45(2):879–85. <https://doi.org/10.1016/j.watres.2010.09.023>.
- Inagaki F, Motomura Y, Ogata S. Microbial silica deposition in geothermal hot waters. *Appl Microbiol Biotechnol*. 2003;60(6):605–11. <https://doi.org/10.1007/s00253-002-1100-y>.
- Ji-Zhou D, Vorkink WP, Lee ML. Origin of long-chain alkylcyclohexanes and alkylbenzenes in a coal-bed wax. *Geochimica et Cosmochimica Acta*. 1993;57(4):837–49. [https://doi.org/10.1016/0016-7037\(93\)90172-5](https://doi.org/10.1016/0016-7037(93)90172-5).
- Kawamura K, Tannenbaum E, Huizinga BJ, Kaplan IR. Volatile organic acids generated from kerogen during laboratory heating. *Geochem J*. 1986;20(1):51–9. <https://doi.org/10.2343/geochemj.20.51>.
- Keim M, Loewer M, Wieland C, Zosseder K, Baumann T, Hackl C, Bauer W, et al. Tiefengeothermie in Bayern. Report, Geothermie-Allianz Bayern; 2020. Accessed: 2021-11-22. <https://mediatum.ub.tum.de/doc/1553803/file.pdf>
- Kharaka YK, Hanor JS. Deep Fluids in the Continents: I. Sedimentary Basins. *Treatise Geochem*. 2003;5:605. <https://doi.org/10.1016/B0-08-043751-6/05085-4>.
- Kharaka YK, Lundegard PD, Giordano TH. Distribution and origin of organic ligands in subsurface waters from sedimentary basins. *Rev Econ Geol*. 2000;9:119–31.
- Kharaka YK, Maest AS, Carothers WW, Law LM, Lamothe PJ, Fries TL. Geochemistry of metal-rich brines from central Mississippi Salt Dome basin, U.S.A. *Appl Geochem*. 1987;2(5):543–61. [https://doi.org/10.1016/0883-2927\(87\)90008-4](https://doi.org/10.1016/0883-2927(87)90008-4) (**Geochemistry of Waters in Deep Sedimentary Basins**).
- Kharaka YK, Hull RW, Carothers WW. Water-Rock Interactions in Sedimentary Basins. In: Gautier, D., Kharaka, Y.K. (eds.) *Relationship of Organic Matter and Mineral Diagenesis*, Society for Sedimentary Geology, Tulsa; 1985a. p. 79–176. <https://doi.org/10.2110/scn.85.03.0079>
- Kharaka YK, Law LM, Carothers WW, Goerlitz DF. Role of Organic Species Dissolved in Formation Waters from Sedimentary Basins in Mineral Diagenesis. In: DL, G (ed.) *Roles of Organic Matter in Sediment Diagenesis*, Soc. Econ. Paleontol. Mineral. Spec. Publ. No. 38, Tulsa; 1985b. p. 111–122. <https://doi.org/10.2110/pec.86.38.0111>
- Kharaka YK, Gunter WD, Aggarwal PK, Perkins EH, DeBaal JD. SOLMINEQ.88; a computer program for geochemical modeling of water-rock interactions. Report 88-4227, U.S. Geological Survey; 1988. <https://doi.org/10.3133/wri884227>
- Kharaka YK, Lundegard PD, Ambats G, Evans WC, Bischoff JL. Generation of aliphatic acid anions and carbon dioxide by hydrous pyrolysis of crude oils. *Appl Geochem*. 1993;8(4):317–24. [https://doi.org/10.1016/0883-2927\(93\)90001-W](https://doi.org/10.1016/0883-2927(93)90001-W).
- Kieft TL, Walters CC, Higgins MB, Mennito AS, Clewett CFM, Heuer V, Pullin MJ, Hendrickson S, van Heerden E, Sherwood Lollar B, Lau MCY, Onstott TC. Dissolved organic matter compositions in 0.6–3.4 km deep fracture waters, Kaapvaal Craton, South Africa. *Org Geochem*. 2018;118:116–31. <https://doi.org/10.1016/j.orggeochem.2018.02.003>.
- Killops S, Killops V. *Introduction to Organic Geochemistry*, 2nd Edn (paperback). Oxford: Blackwell Science Ltd; 2005.
- Kloppmann W, Négrel P, Casanova J, Klinge H, Schelkes K, Guerrot C. Halite dissolution derived brines in the vicinity of a Permian salt dome (in German basin). Evidence from boron, strontium, oxygen, and hydrogen isotopes. *Geochimica et Cosmochimica Acta*. 2001;65(22):4087–101. [https://doi.org/10.1016/S0016-7037\(01\)00640-8](https://doi.org/10.1016/S0016-7037(01)00640-8).
- Kompanichenko VN, Poturay VA, Karpov GA. Organic compounds in thermal water: the Mutnovskii area and the Uzon caldera. *J Volcanol Seismol*. 2016;10(5):305–19. <https://doi.org/10.1134/S0742046316050031>.
- Konn C, Testemale D, Querellou J, Holm NG, Charlou J-L. New insight into the contributions of thermogenic processes and biogenic sources to the generation of organic compounds in hydrothermal fluids. *Geobiology*. 2011;9(1):79–93. <https://doi.org/10.1111/j.1472-4669.2010.00260.x>.
- Kovacs K, Gaspar A, Sajgó C, Schmitt-Kopplin P, Tombacz E. Comparative study on humic substances isolated in thermal groundwaters from deep aquifers below 700 m. *Geochem J*. 2012;46(3):211–24. <https://doi.org/10.2343/geochemj.1.0168>.
- Kulakov V. Geological, structural and geothermal conditions for the formation of thermal groundwater in the Amur Region. *Pac Geol*. 2014;33(5):66–79.
- Kárpáti Z, Sajgó C, Vető I, Klopp G, Horváth I. Organic matter in thermal waters of the Pannonian Basin—a preliminary report on aromatic compounds. presented at the 17th international meeting on organic geochemistry, environmental organic geochemistry session, donostia-san sebastian, spain, 4-8 september, 1995.1. *Org Geochem*. 1999;30(7):701–12. [https://doi.org/10.1016/S0146-6380\(99\)00006-6](https://doi.org/10.1016/S0146-6380(99)00006-6).
- Lang SQ, Butterfield DA, Schulte M, Kelley DS, Lilley MD. Elevated concentrations of formate, acetate and dissolved organic carbon found at the Lost City hydrothermal field. *Geochimica et Cosmochimica Acta*. 2010;74(3):941–52. <https://doi.org/10.1016/j.gca.2009.10.045>.
- Le Carlier C, Royer J-J, Flores E. Convective heat transfer at the Soultz-sous-Forets Geothermal Site: implications for oil potential. *First Break*. 1994;12(11).
- Ledésert B, Joffre J, Amblès A, Sardini P, Genter A, Meunier A. Organic matter in the Soultz HDR granitic thermal exchanger (France): natural tracer of fluid circulations between the basement and its sedimentary cover. *J Volcanol Geotherm Res*. 1996;70(3):235–53. [https://doi.org/10.1016/0377-0273\(95\)00058-5](https://doi.org/10.1016/0377-0273(95)00058-5).
- Leenheer J, Malcolm R, McKinley P, Eccles L. Occurrence of dissolved organic carbon in selected ground-water samples in the United States. *J Res US Geol Surv*. 1974;2(3):361–9.
- Leins A, Vieth-Hillebrand A, Bregnard D, Günther K, Junier P, Regenspurg S. Dissolved organic compounds in geothermal fluids used for energy production. *GFZ Data Services*; 2022. <https://doi.org/10.5880/GFZ.4.8.2022.001>
- Lovley DR, Chapelle FH. Deep subsurface microbial processes. *Rev Geophys*. 1995;33(3):365–81. <https://doi.org/10.1029/95RG01305>.
- Lovley DR, Klug MJ. Model for the distribution of sulfate reduction and methanogenesis in freshwater sediments. *Geochimica et Cosmochimica Acta*. 1986;50(1):11–8. [https://doi.org/10.1016/0016-7037\(86\)90043-8](https://doi.org/10.1016/0016-7037(86)90043-8).

- Lovley DR, Phillips EJP. Requirement for a microbial consortium to completely oxidize glucose in Fe(III)-reducing sediments. *Appl Environ Microbiol.* 1989;55(12):3234–6. <https://doi.org/10.1128/aem.55.12.3234-3236.1989>.
- Lundegard PD, Kharaka YK. Geochemistry of organic acids in subsurface waters: field data, experimental data, and models. In: *Chemical Modeling of Aqueous Systems II*, ACS Publications, Washington; 1990. p. 169–189. Chap. 13. <https://doi.org/10.1021/bk-1990-0416.ch013>
- Lundegard PD, Kharaka YK. Distribution and Occurrence of Organic Acids in Subsurface Waters. In: *Organic Acids in Geological Processes*, Springer, Heidelberg; 1994. p. 40–69. https://doi.org/10.1007/978-3-642-78356-2_3
- Lundegard PD, Land LS. Carbon Dioxide and Organic Acids: Their Role in Porosity Enhancement and Cementation, Paleogene of the Texas Gulf Coast. In: Gautier DL (ed) *Roles of Organic Matter in Sediment Diagenesis*, pp. 129–146. Soc. Econ. Paleont. Mineral. Spec. Publ. No. 38, Tulsa; 1985. <https://doi.org/10.2110/pec.86.38.0129>
- Lüders V, Plessen B, Romer RL, Weise SM, Banks DA, Hoth P, Dulski P, Schettler G. Chemistry and isotopic composition of Rotliegend and Upper Carboniferous formation waters from the North German Basin. *Chem Geol.* 2010;276(3):198–208. <https://doi.org/10.1016/j.chemgeo.2010.06.006>.
- MacGowan DB, Surdam RC. Difunctional carboxylic acid anions in oilfield waters. *Org Geochem.* 1988;12(3):245–59. [https://doi.org/10.1016/0146-6380\(88\)90262-8](https://doi.org/10.1016/0146-6380(88)90262-8).
- MacGowan DB, Surdam RC. Importance of Organic–Inorganic Reactions to Modeling Water–Rock Interactions During Progressive Clastic Diagenesis. In: *Chemical Modeling of Aqueous Systems II* vol. 416, ACS Publications, Washington; 1990. p. 494–507. Chap. 38. <https://doi.org/10.1021/bk-1990-0416.ch038>
- Mayrhofer C, Niessner R, Baumann T. Hydrochemistry and hydrogen sulfide generating processes in the Malm aquifer, Bavarian Molasse Basin, Germany. *Hydrogeol J.* 2014;22(1):151–62. <https://doi.org/10.1007/s10040-013-1064-2>.
- McCollom TM, Seewald JS. Abiotic synthesis of organic compounds in deep-sea hydrothermal environments. *Chem Rev.* 2007;107(2):382–401. <https://doi.org/10.1021/cr0503660>.
- McCollom TM, Seewald JS, Simoneit BRT. Reactivity of monocyclic aromatic compounds under hydrothermal conditions. *Geochimica et Cosmochimica Acta.* 2001;65(3):455–68. [https://doi.org/10.1016/S0016-7037\(00\)00533-0](https://doi.org/10.1016/S0016-7037(00)00533-0).
- Means JL, Hubbard N. Short-chain aliphatic acid anions in deep subsurface brines: a review of their origin, occurrence, properties, and importance and new data on their distribution and geochemical implications in the Palo Duro Basin, Texas. *Org Geochem.* 1987;11(3):177–91. [https://doi.org/10.1016/0146-6380\(87\)90021-0](https://doi.org/10.1016/0146-6380(87)90021-0).
- Moeller P, Weise S, Tesmer M, Dulski P, Pekdeger A, Bayer U, Magri F. Salinization of groundwater in the North German Basin: results from conjoint investigation of major, trace element and multi-isotope distribution. *Int J Earth Sci.* 2008;97(5):1057–73. <https://doi.org/10.1007/s00531-007-0211-1>.
- Mouchot J, Genter A, Cuenot N, Scheiber J, Seibel O, Bosia C, Ravier G, Mouchot J, Genter A, Cuenot N, et al. First year of operation from EGS geothermal plants in Alsace, France: scaling issues. Proceedings of the 43rd Workshop on Geothermal Reservoir Engineering Stanford University, Stanford, California, February 12–14, 2018; 2018.
- Nachtmann W, Wagner L. Mesozoic and early tertiary evolution of the Alpine foreland in upper Austria and Salzburg, Austria. *Tectonophysics.* 1987;137(1):61–76. [https://doi.org/10.1016/0040-1951\(87\)90314-3](https://doi.org/10.1016/0040-1951(87)90314-3) (**Compressional Intra-Plate Deformations in the Alpine Foreland**).
- Neumann E. Hydrogeologische Verhältnisse des Paläozoikums und Mesozoikums am Nordrand der Norddeutsch-Polnischen Senke und ihre Beziehungen zu den Erdöl- und Erdgasvorkommen [Hydrogeological settings of the Palaeozoic and Mesozoic strata in respect to the oil and gas resources at the northern boundary of the German-Polish basin]. PhD thesis, Bergakademie Freiberg, Germany; 1975.
- Norini G, Groppelli G, Sulpizio R, Carrasco-Núñez G, Dávila-Harris P, Pelliccioli C, Zucca F, De Franco R. Structural analysis and thermal remote sensing of the Los Humeros Volcanic Complex: Implications for volcano structure and geothermal exploration. *J Volcanol Geotherm Res.* 2015;301:221–37. <https://doi.org/10.1016/j.jvolgeores.2015.05.014>.
- Norini G, Carrasco-Núñez G, Corbo-Camargo F, Lermo J, Rojas JH, Castro C, Bonini M, Montanari D, Corti G, Moratti G, Piccardi L, Chavez G, Zuluaga MC, Ramirez M, Cedillo F. The structural architecture of the Los Humeros volcanic complex and geothermal field. *J Volcanol Geotherm Res.* 2019;381:312–29. <https://doi.org/10.1016/j.jvolgeores.2019.06.010>.
- Novak JT, Ramesh MS. Stimulation in anaerobic degradation. *Water Res.* 1975;9(11):963–7. [https://doi.org/10.1016/0043-1354\(75\)90124-4](https://doi.org/10.1016/0043-1354(75)90124-4).
- Otten C. Charakterisierung eines organischen Scalinginhibitors und dessen Abbauprodukte mit Hilfe verschiedener Analyseverfahren. Master's thesis, Hochschulbibliothek, Hochschule Merseburg; 2019. <https://doi.org/10.25673/14058>
- Pauwels H, Fouillac C, Fouillac A-M. Chemistry and isotopes of deep geothermal saline fluids in the Upper Rhine Graben: origin of compounds and water-rock interactions. *Geochimica et Cosmochimica Acta.* 1993;57(12):2737–49. [https://doi.org/10.1016/0016-7037\(93\)90387-C](https://doi.org/10.1016/0016-7037(93)90387-C).
- Peiffer L, Carrasco-Núñez G, Mazot A, Villanueva-Estrada RE, Inguaggiato C, Bernard Romero R, Rocha Miller R, Hernández Rojas J. Soil degassing at the Los Humeros geothermal field (Mexico). *J Volcanol Geotherm Res.* 2018;356:163–74. <https://doi.org/10.1016/j.jvolgeores.2018.03.001>.
- Pelekani C, Newcombe G, Snoeyink VL, Hepplewhite C, Assemi S, Beckett R. Characterization of natural organic matter using high performance size exclusion chromatography. *Environ Sci Technol.* 1999;33(16):2807–13. <https://doi.org/10.1021/es9901314>.
- Penru Y, Simon FX, Guastalli AR, Esplugas S, Llorens J, Baig S. Characterization of natural organic matter from Mediterranean coastal seawater. *J Water Supply Res Technol Aqua.* 2013;62(1):42–51. <https://doi.org/10.2166/aqua.2013.113>.
- Pinti DL, Castro MC, Lopez-Hernandez A, Han G, Shouakar-Stash O, Hall CM, Ramírez-Montes M. Fluid circulation and reservoir conditions of the Los Humeros geothermal field (LHGF), Mexico, as revealed by a noble gas survey. *J Volcanol Geotherm Res.* 2017;333–334:104–15. <https://doi.org/10.1016/j.jvolgeores.2017.01.015>.
- Poturay VA. Organic matter in ground- and surface waters in the area of the Annenskii geothermal field, Russian Far East. *Geochem Int.* 2017;55(4):393–400. <https://doi.org/10.1134/S0016702917020057>.

- Poturay V, Kompanichenko V. Composition and distribution of saturated hydrocarbons in the thermal waters and vapor-water mixture of the Mutnovskii geothermal field and Uzon caldera, Kamchatka. *Geochem Int.* 2019;57(1):74–82. <https://doi.org/10.1134/S0016702919010087>.
- Pribnow D, Schellschmidt R. Thermal tracking of upper crustal fluid flow in the Rhine graben. *Geophys Res Lett.* 2000;27(13):1957–60. <https://doi.org/10.1029/2000GL008494>.
- Pytlak Ł, Leis A, Prochaska W, Sachsenhofer R, Gross D, Linzer H-G. Light hydrocarbon geochemistry of oils in the alpine Foreland basin: Impact of geothermal fluids on the petroleum system. *Geofluids.* 2017;2017.
- Reeves EP, Fiebig J. Abiotic synthesis of methane and organic compounds in Earth's lithosphere. *Elements.* 2020;16(1):25–31. <https://doi.org/10.2138/gselements.16.1.25>.
- Regenspurg S, Wiersberg T, Brandt W, Huenges E, Saadat A, Schmidt K, Zimmermann G. Geochemical properties of saline geothermal fluids from the in-situ geothermal laboratory Groß Schönebeck (Germany). *Geochemistry.* 2010;70:3–12. <https://doi.org/10.1016/j.chemer.2010.05.002> (**Geoenergy: From Visions to Solutions**).
- Regenspurg S, Feldbusch E, Byrne J, Deon F, Driba DL, Henningses J, Kappler A, Naumann R, Reinsch T, Schubert C. Mineral precipitation during production of geothermal fluid from a Permian Rotliegend reservoir. *Geothermics.* 2015;54:122–35. <https://doi.org/10.1016/j.geothermics.2015.01.003>.
- Regenspurg S, Feldbusch E, Norden B, Tichomirowa M. Fluid-rock interactions in a geothermal Rotliegend/Permo-Carboniferous reservoir (North German Basin). *Appl Geochem.* 2016;69:12–27. <https://doi.org/10.1016/j.apgeochem.2016.03.010>.
- Regenspurg S, Alawi M, Blöcher G, Börper M, Kranz S, Norden B, Saadat A, Scheytt T, Virchow L, Vieth-Hillebrand A. Impact of drilling mud on chemistry and microbiology of an Upper Triassic groundwater after drilling and testing an exploration well for aquifer thermal energy storage in Berlin (Germany). *Environ Earth Sci.* 2018;77(13):516. <https://doi.org/10.1007/s12665-018-7696-8>.
- Reinsch T, Dobson P, Asanuma H, Huenges E, Poletto F, Sanjuan B. Utilizing supercritical geothermal systems: a review of past ventures and ongoing research activities. *Geotherm Energy.* 2017;5(1):1–25. <https://doi.org/10.1186/s40517-017-0075-y>.
- Reinsel MA, Borkowski JJ, Sears JT. Partition coefficients for acetic, propionic, and butyric acids in a crude oil/water system. *J Chem Eng Data.* 1994;39(3):513–6. <https://doi.org/10.1021/je00015a026>.
- Rieke H, Kossow D, McCann T, Krawczyk C. Tectono-sedimentary evolution of the northernmost margin of the NE German Basin between uppermost Carboniferous and Late Permian (Rotliegend). *Geol J.* 2001;36(1):19–37. <https://doi.org/10.1002/gj.873>.
- Sachsenhofer RF, Leitner B, Linzer H-G, Bechtel A, Ćorić S, Gratzner R, Reischenbacher D, Soliman A. Deposition, erosion and hydrocarbon source potential of the Oligocene Eggerding Formation (Molasse Basin, Austria). *Austrian J Earth Sci.* 2010;103(1):76–99.
- Sachsenhofer R, Schulz H-M. Architecture of Lower Oligocene source rocks in the Alpine Foreland Basin: a model for syn- and post-depositional source-rock features in the Paratethyan realm. *Petroleum Geosci.* 2006;12(4):363–77. <https://doi.org/10.1144/1354-079306-712>.
- Saemundsson K, Axelsson G, Steingrímsson B. Geothermal systems in global perspective. Short course on exploration for geothermal resources, UNU GTP. 2009;11.
- Sand W. Microbial life in geothermal waters. *Geothermics.* 2003;32(4):655–67. [https://doi.org/10.1016/S0375-6505\(03\)00058-0](https://doi.org/10.1016/S0375-6505(03)00058-0) (**Selected Papers from the European Geothermal Conference 2003**).
- Sanjuan B, Millot R, Ásmundsson R, Brach M, Giroud N. Use of two new Na/Li geothermometric relationships for geothermal fluids in volcanic environments. *Chem Geol.* 2014;389:60–81. <https://doi.org/10.1016/j.chemgeo.2014.09.011>.
- Sanjuan B, Millot R, Innocent C, Dezayes C, Scheiber J, Brach M. Major geochemical characteristics of geothermal brines from the Upper Rhine Graben granitic basement with constraints on temperature and circulation. *Chem Geol.* 2016;428:27–47. <https://doi.org/10.1016/j.chemgeo.2016.02.021>.
- Sanjuan B, Millot R, Dezayes C, Brach M. Main characteristics of the deep geothermal brine (5km) at Soultz-sous-Forêts (France) determined using geochemical and tracer test data. *Comptes Rendus Geoscience.* 2010;342(7):546–59. <https://doi.org/10.1016/j.crte.2009.10.009>.
- Schad A. Das Erdölfeld Landau. *Abh Geol Landesamt Baden-Württemberg.* 1962;4:81–101.
- Scheck M, Barrio-Alvers L, Bayer U, Götze H-J. Density structure of the Northeast German basin: 3D modelling along the DEKORP line BASIN96. *Phys Chem Earth Part A Solid Earth Geodesy.* 1999;24(3):221–30. [https://doi.org/10.1016/S1464-1895\(99\)00022-8](https://doi.org/10.1016/S1464-1895(99)00022-8).
- Scheiber J, Seibt A, Jähnichen S, Degering D, Mouchot J. Combined Application of Inhibitors for Scale and Corrosion Mitigation: Lessons Learned. *Proceedings of the European Geothermal Congress, Den Haag, The Netherlands, 11–14 June, 2019; 2019.*
- Schellschmidt R, Clauser C. The thermal regime of the Upper Rhine Graben and the anomaly at Soultz. *Zeitschrift für Angewandte Geologie.* 1996;42(1):40–4.
- Seewald JS. Model for the origin of carboxylic acids in basinal brines. *Geochimica et Cosmochimica Acta.* 2001;65(21):3779–89. [https://doi.org/10.1016/S0016-7037\(01\)00702-5](https://doi.org/10.1016/S0016-7037(01)00702-5).
- Seibt A, Hoth P, Naumann D. Gas solubility in formation waters of the North German Basin—implications for geothermal energy recovery. *Proceedings World Geothermal Congress, May 28 - June 10, 2000, Kyushu - Tohoku, Japan; 2000.*
- Seibt P, Wolfgramm M. Practical experience in the reinjection of thermal waters into sandstone. *Proceedings of the Workshop for decision makers on direct heating use of geothermal resources in Asia. 11–18 May, 2008, Tianjin, China; 2008.*
- Seibt P, Kabus F, Hoth P. The Neustadt-Glewe Geothermal Power Plant - Practical Experience in the Reinjection of Cooled Thermal Waters into Sandstone Aquifers. *Proceedings World Geothermal Conference; 2005.*
- Sherwood Lollar B, Heuer VB, McDermott J, Tille S, Warr O, Moran JJ, Telling J, Hinrichs K-U. A window into the abiotic carbon cycle—acetate and formate in fracture waters in 2.7 billion year-old host rocks of the Canadian Shield. *Geochimica et Cosmochimica Acta.* 2021;294:295–314. <https://doi.org/10.1016/j.gca.2020.11.026>.
- Simoneit BRT. Aqueous high-temperature and high-pressure organic geochemistry of hydrothermal vent systems. *Geochimica et Cosmochimica Acta.* 1993;57(14):3231–43. [https://doi.org/10.1016/0016-7037\(93\)90536-6](https://doi.org/10.1016/0016-7037(93)90536-6).

- Simoneit BRT, Deamer DW, Kompanichenko V. Characterization of hydrothermally generated oil from the Uzon caldera, Kamchatka. *Appl Geochem*. 2009;24(2):303–9. <https://doi.org/10.1016/j.apgeochem.2008.10.007> (**Natural Low-pH Environments Unaffected by Human Activity**).
- Simoneit BRT, Lein AY, Peresyphkin VI, Osipov GA. Composition and origin of hydrothermal petroleum and associated lipids in the sulfide deposits of the Rainbow field (Mid-Atlantic Ridge at 36°N), Associate editor: G. A. Logan. *Geochimica et Cosmochimica Acta*. 2004;68(10):2275–94. <https://doi.org/10.1016/j.gca.2003.11.025>.
- Siskin M, Katritzky AR. Reactivity of organic compounds in hot water: geochemical and technological implications. *Science*. 1991;254(5029):231–7. <https://doi.org/10.1126/science.254.5029.231>.
- Sørensen J, Christensen D, Jørgensen BB. Volatile fatty acids and hydrogen as substrates for sulfate-reducing bacteria in anaerobic marine sediment. *Appl Environ Microbiol*. 1981;42(1):5–11. <https://doi.org/10.1128/aem.42.1.5-11.1981>.
- Steintherme.de: Zusammensetzung der Sole. <https://www.steintherme.de/thermalsole/zusammensetzung/> accessed 2021-11-18; 2021.
- Stichler W, Rauer W, Weise S, Wolf M, Koschel G, Stier P, Prestel R, Hedin K, Bertleff B. Isotopenhydrologische und hydrochemische Untersuchungen zur Erkundung des Fließsystems im Malmkarstaquifer des süddeutschen Alpenvorlandes. *Zeitschrift der Deutschen Geologischen Gesellschaft*. 1987;138(2):387–98. <https://doi.org/10.1127/zdgg/138/1987/387>.
- Strauss J, Schirmeister L, Mangelsdorf K, Eichhorn L, Wetterich S, Herzsich U. Organic-matter quality of deep permafrost carbon - a study from Arctic Siberia. *Biogeosciences*. 2015;12(7):2227–45. <https://doi.org/10.5194/bg-12-2227-2015>.
- Surdam RC, Boese SW, Crosse LJ. The chemistry of secondary porosity. In: McDonald DA, Surdam RC, editors. *Clastic diagenesis*. Tulsa: American Association of Petroleum Geologists; 1984. p. 127–50. <https://doi.org/10.1306/M37435C8>.
- Sánchez-Avila JI, García-Sánchez BE, Vara-Castro GM, Kretzschmar T. Distribution and origin of organic compounds in the condensates from a Mexican high-temperature geothermal field. *Geothermics*. 2021;89:101980. <https://doi.org/10.1016/j.geothermics.2020.101980>.
- Takai K, Nakamura K, Toki T, Tsunogai U, Miyazaki M, Miyazaki J, Hirayama H, Nakagawa S, Nunoura T, Horikoshi K. Cell proliferation at 122° C and isotopically heavy CH₄ production by a hyperthermophilic methanogen under high-pressure cultivation. *Proc Natl Acad Sci*. 2008;105(31):10949–54. <https://doi.org/10.1073/pnas.0712334105>.
- Tassi F, Venturi S, Cabassi J, Capecciacci F, Nisi B, Vaselli O. Volatile organic compounds (VOCs) in soil gases from Solfatara crater (Campi Flegrei, southern Italy): Geogenic source(s) vs. biogeochemical processes. *Appl Geochem*. 2015;56:37–49. <https://doi.org/10.1016/j.apgeochem.2015.02.005>.
- Tesmer M, Moeller P, Wieland S, Jahnke C, Voigt H, Pekdeger A. Deep reaching fluid flow in the North East German Basin: origin and processes of groundwater salinisation. *Hydrogeol J*. 2007;15(7):1291–306. <https://doi.org/10.1007/s10040-007-0176-y>.
- Thomas MM, Clouse JA, Longo JM. Adsorption of organic compounds on carbonate minerals: 1. Model compounds and their influence on mineral wettability. *Chem Geol*. 1993;109(1):201–13. [https://doi.org/10.1016/0009-2541\(93\)90070-Y](https://doi.org/10.1016/0009-2541(93)90070-Y).
- Thurman E. Amount of organic carbon in natural waters. *Org Geochem Nat Waters*. 1985. https://doi.org/10.1007/978-94-009-5095-5_2.
- tiefengeothermie.de: Insheim. <https://www.tiefengeothermie.de/projekte/insheim> accessed 2021-11-23; 2021a.
- tiefengeothermie.de: Rittershoffen/ECOGI. <https://www.tiefengeothermie.de/projekte/rittershoffen-ecogi> accessed 2021-11-23; 2021b.
- Varsányi I, Kovács LO, Kárpáti Z, Matray J-M. Carbon forms in formation waters from the Pannonian Basin, Hungary. *Chem Geol*. 2002;189(3):165–82. [https://doi.org/10.1016/S0009-2541\(02\)00103-1](https://doi.org/10.1016/S0009-2541(02)00103-1).
- Vetter A. The influence of geothermal plants on the biogeochemistry of the microbial ecosystems in aquifers. Doctoral thesis, Technische Universität Berlin, Fakultät VI - Planen Bauen Umwelt, Berlin; 2012. <https://doi.org/10.14279/depositonnce-3419>
- Vidal J, Genter A. Overview of naturally permeable fractured reservoirs in the central and southern Upper Rhine Graben: insights from geothermal wells. *Geothermics*. 2018;74:57–73. <https://doi.org/10.1016/j.geothermics.2018.02.003>.
- Voigt H. Zur Dynamik mineralisierter Schichtenwässer. *Zeitschrift angewandte Geologie*. 1975;21(4).
- Vosteen H-D, Rath V, Schmidt-Mumm A, Clauser C. The thermal regime of the Northeastern-German Basin from 2-D inversion. *Tectonophysics*. 2004;386(1):81–95. <https://doi.org/10.1016/j.tecto.2004.05.004>.
- Wessely G. Zur Geologie und Hydrodynamik im südlichen Wiener Becken und seiner Randzone. *Mitteilungen der österreichischen Geologischen Gesellschaft*. 1983;76:27–68.
- Westphal A, Eichinger F, Eichinger L, Würdemann H. Change in the microbial community of saline geothermal fluids amended with a scaling inhibitor: effects of heat extraction and nitrate dosage. *Extremophiles*. 2019;23(3):283–304. <https://doi.org/10.1007/s00792-019-01080-0>.
- Wolfgramm M, Seibt A. Zusammensetzung von Tiefenwässern in Deutschland und ihre Relevanz für geothermische Anlagen. *GtV-Tagung in Karlsruhe 2008*; 2008.
- You C-F, Gieskes JM. Hydrothermal alteration of hemi-pelagic sediments: experimental evaluation of geochemical processes in shallow subduction zones. *Appl Geochem*. 2001;16(9):1055–66. [https://doi.org/10.1016/S0883-2927\(01\)00024-5](https://doi.org/10.1016/S0883-2927(01)00024-5).
- Zekiri F. Erstellung von Temperaturkarten in verschiedenen Tiefen im südlichen Wiener Becken. PhD thesis, Universität Wien; 2011. <https://doi.org/10.25365/thesis.14913>
- Zhu Y, Vieth-Hillebrand A, Wilke FDH, Horsfield B. Characterization of water-soluble organic compounds released from black shales and coals. *Int J Coal Geol*. 2015;150–151:265–75. <https://doi.org/10.1016/j.coal.2015.09.009>.
- Zotzmann J, Vetter A, Regenspurg S. Evaluating efficiency and stability of calcite scaling inhibitors at high pressure and high temperature in laboratory scale. *Geotherm Energy*. 2018;6(1):18. <https://doi.org/10.1186/s40517-018-0105-4>.

Publisher's Note

Springer Nature remains neutral with regard to jurisdictional claims in published maps and institutional affiliations.

Submit your manuscript to a SpringerOpen[®] journal and benefit from:

- ▶ Convenient online submission
- ▶ Rigorous peer review
- ▶ Open access: articles freely available online
- ▶ High visibility within the field
- ▶ Retaining the copyright to your article

Submit your next manuscript at ▶ [springeropen.com](https://www.springeropen.com)
